Antenna Packing in Low Power Systems: Communication Limits and Array Design*

Tarik Muharemovic, Ashutosh Sabharwal and Behnaam Aazhang
Dept. of Electrical and Computer Engineering
Rice University, Houston, TX 77005
{tarik,ashu,aaz}@rice.edu

Abstract

In this paper, we study design of transceiver antenna arrays and its impact on spectral efficiency of low-power systems. Our primary motivation is construction of practical and portable multi-antenna configurations with a very small and a-priori fixed volume for placing antennas. Using spectral efficiency as a target metric for array optimization, we show that any array configuration, transmit or receive, can be characterized via a parameter that we interpret as "effective degrees of freedom." For any array configuration, effective degrees of freedom describes an equivalent uncorrelated array, which results in the same low-power behavior of spectral efficiency.

Joint optimization of transmit and receive antenna configurations decouples into maximizing effective degrees of freedom for transmitter and receiver separately. To achieve this goal, we introduce and study a theoretical benchmark of "limiting degrees of freedom," which is the least upper bound on effective degrees of freedom, evaluated over all configurations with finite number of antennas. Limiting degrees of freedom therefore describes the best possible performance for any transceiver array which confines its elements inside a given space. We compute a closed-form expression for limiting degrees of freedom of a circular geometry. Finally, we present numerical procedure and examples for designing linear and square arrays with non-uniform spacing, which typically exhibit significant spectral efficiency gains over uniform arrays.

*This work was supported in part by NSF Grant CCR-0311398, and presented at the Forty-Second Annual Allerton Conference on Communication, Control, and Computing in September 2004.

1 Introduction

Capacity gains which are made possible using transmit and receive antenna arrays are vastly appreciated in the current literature [1, 2, 6–8, 10, 11]. Motivated by large capacity improvements, various scientific contributions from the last decade focus on concrete transmission and reception strategies using multiple antennas; a sampling of major issues is found in [4]. Numerous contributions have further perpetuated the introduction of multiple antenna solutions into ever-emerging wireless standards. Till present date, both theoretic and practical work on multiantenna arrays have focused on either analyzing or achieving the capacity of fixed antenna configurations. Although the analysis of fixed antenna configurations may be used for synthesizing optimal antenna configurations, very little is known regarding where and how many antennas should be placed, given that transceiver volume for the array is determined a-priori. In this paper, we address how capacity optimizing antenna arrays should be designed, and we derive communication limits which govern them, when only spatial geometry for placing antennas is fixed.

Conventional design wisdom for obtaining nearly uncorrelated antennas and near-maximum capacity is to space the array elements sufficiently apart. Such design rule is completely valid, and is fully supported by our analysis. The utility of the framework in this paper lies in analysis and design of portable arrays with a number of elements in a limited space, where arbitrary element separation is not an option. The challenge in designing such arrays, as will become clear in the main body, stems from highly complicated relation between antenna locations and the resulting array correlation, which is governed by the Bessel function of zeroth order [5, 13]. Non-trivial relation between the array configuration and it correlation causes that uniformly spaced arrays are often not the optimal choices for small apertures.

In order to address capacity optimizing configurations, this work initially considers a system where both transmitter and receiver are only constrained by disjoint spatial volumes for antenna positioning, and not by the actual number of elements. Our exposition will be guided by following questions in particular. First, what are the spectral efficiency limitations which can be achieved by the above system, and what is the impact of the restricted spatial volume? Second, how should actual finite antenna arrays be designed, in order to maximize their capacity limits? The later question undoubtedly has more practical appeal, but we believe that it cannot be addressed appropriately without initial thorough understanding of various limits and tradeoffs which are imposed by a fixed transceiver volume. Naturally, as more antennas are packed inside a restricted volume, the increase in mutual antenna correlation becomes inevitable. As we show in the main body, such increase of antenna correlation will offset capacity benefits of multiantenna transmission up to the point of saturation.

Our work applies to multiantenna transceivers in the low power communication mode, where spectral efficiency R and energy per information bit[1] $\mathcal{E}$ represent key measures of the overall system performance [3, 7, 20]. We note that spectral efficiency of low-power antenna arrays, along with the impact of antenna correlation, were studied in [3] and [7] respectively. In particular, authors of [7] consider fixed arrays and introduce the "correlation number," as a parameter which measures the cumulative effect of a correlated antenna configuration. Correlation number, however, is not suitable for analysis of arrays

[1]Other authors [3, 7, 20] refer to $\mathcal{E}$ as EbN0, but we prefer a simple single-character notation $\mathcal{E}$. Noise variance N0 is normalized to unity per each complex dimension.

with increasing number of antennas, because it also grows without bounds when more antennas are packed inside a given volume.

In order to address configurations with growing number of elements, which are also referred to as dense multiantenna arrays [11], we will introduce and study a convergent array parameter: the "effective degrees of freedom." Effective degrees of freedom will be derived directly from low-power approximation to spectral efficiency, and will serve as a convenient characterization of an antenna configuration. For any given transmit or receive array, effective degrees of freedom measures number of antennas in the equivalent uncorrelated array, which achieves the same spectral efficiency. Consecutively, effective degrees of freedom is a parameter which ought to be maximized through appropriate configuration design. Namely, any transmit or receive array design which maximizes the effective degrees of freedom, will also maximize the spectral efficiency. Furthermore, we note how effective degrees of freedom provides a convenient method to compare different antenna configurations which can have arbitrary number of antennas.

Given a transceiver volume with unrestricted number of antenna elements, two basic competing effects will occur. First, as the number of antennas starts to grow, it is intuitive to expect certain capacity benefits, which we interpret as increase in effective degrees of freedom for the array. On the other hand, the opposing effect is provided by the mutual antenna correlation, which comes from the limited transceiver space, and which now results in the reduction of effective degrees of freedom. To strike the balance of these two competing effects, we introduce a theoretical benchmark: the "limiting degrees of freedom." Limiting degrees of freedom is defined as the least upper bound to the effective degrees of freedom, evaluated over all antenna configurations which are confined to a given transceiver volume. Thus, the limiting degrees of freedom is only a function of a given aperture for mounting antennas, and not any particular antenna configuration.

After introducing the limiting degrees of freedom, we proceed with a study of its fundamental characteristics. We note that limiting degrees of freedom can be interpreted as a sub-additive set function (measure) on subsets of $\mathbb{R}^3$, with the following intuitive properties. First, it is lower bounded by one, simply because one can do no worse than placing a single antenna inside a given volume. Second, it is monotone, which means that a larger space always offers more limiting degrees of freedom. Third, it is shown that if volume $G \subseteq \mathbb{R}^3$ can be partitioned as $G = G_1 \cup G_2$ where G_1 and G_2 are sufficiently separated, than limiting degrees of freedom for G is computed by adding limiting degrees of freedom for the components G_1 and G_2. Most importantly, we show that any bounded transceiver volume always offers only finitely many limiting degrees of freedom, which proves a saturation effect for effective degrees of freedom, and ultimately, for the spectral efficiency. We will show how to make use of limiting degrees of freedom (d.o.f.) as a systematic basis for comparison of antenna configurations.

Finally, we utilize the proposed analysis tools to synthesize antenna configurations for three common array geometries: circular, linear and square. For the circular array, we compute the limiting d.o.f. in a closed form, and also derive a small array approximation, which has the potential use for small sized low-power sensor nodes. A surprising discovery is that for small size circular arrays, the increase in limiting d.o.f. is in fact quadratic in the radius of the array. However, as radius of the array grows further, the number of available d.o.f. appears to only increase linearly with the radius; this result is consistent with the known signal space approach in [10]. On the other hand, for linear and square geometries, finding closed form expressions for limiting d.o.f. appears to be intractable.

However, effective d.o.f. can be computed easily, and thus we propose a simple greedy algorithm for optimizing the location of antennas. We demonstrate that in almost all cases, uniform spacing can be significantly improved upon.

We next give an overview of related results which consider different aspects of the array packing problem. Pollock, Abhayapala and Kennedy in [8] show that channel capacity exhibits saturation effect when more antennas are uniformly packed on the circle boundary. Work in [8] focuses on uniform circular arrays, and concludes with the conjecture[2] that limits provided therein hold valid for arbitrary circular arrays. In [9], same authors also provide an upper bound for the mutual information, by finding the number of communication modes which are governed by different solutions of Maxwell's equations. Ada and Tse in [10] take the signal space approach, and define number of "spatial degrees of freedom" to be the number of basis functions which span the antenna array response. The basis contains approximately $4\pi r/\lambda$ functions for the large circle geometry, where r is the circle radius and λ is the carrier wavelength. Chiurtu, Rimoldi and Telatar in [11] consider channel model which incorporates the effects of antenna coupling. As shown in [11], transmit antenna coupling tends to increase the average transmitted power for spatially correlated signaling strategies. Similar to [8], Gesbert in [12] assumes a uniform circular array, and points out that one method to model the antenna coupling is to simply alter the Bessel antenna correlation function J_0.

The outline for the rest of the paper is as follows. In Section 2, we introduce our channel and antenna model, and review already known results for spectral efficiency in the low-power regime. In Section 3, we derive spectral efficiency for correlated antenna arrays under isotropically invariant fading, and introduce and study the concept of effective degrees of freedom. In Section 4, we study limiting degrees of freedom and derive limiting d.o.f. for a circular array. Numerical design examples are studied in Section 5, and we conclude in Section 6.

2 System Model and Preliminaries

2.1 Channel and Antenna Model

We consider the linear multi-antenna channel

$$Y = \mathcal{H}X + \eta, \tag{1}$$

where vector X contains symbols which are transmitted over N antennas, and vector Y contains symbols which are received by M antennas. Entry $\mathcal{H}(m,n)$ represents the propagation coefficient from $n-$th transmit to $m-$th receive antenna. Additive noise η is assumed to be independent and identically distributed complex AWGN, which is normalized to unit variance for each complex dimension, i.e. $\mathrm{E}\left[\eta\eta^\dagger\right] = \mathrm{I}_{\mathrm{M}\times\mathrm{M}}$. Furthermore, we also assume spatially uncorrelated signalling, where transmit symbols X are modeled as independent[3] and identically distributed complex Gaussian.

[2] Section 4.2 provides a proof of this conjecture from [8].

[3] We consider only i.i.d. signalling for following three reasons. First, it is overwhelmingly prevalent in practice. Second, it results in one design criterion for both transmit and receive arrays, which is shown in the main paper body, and which is convenient since one array may serve for both uplink and downlink. Third, this approach is in line with other works [7, 15] on correlated multiantenna systems, thereby allowing direct comparisons.

According to [5–7], the standard method to model correlation between transmit and receive antennas is to set

$$\mathcal{H} = \Phi^{\frac{1}{2}}\widehat{\mathcal{H}}\Theta^{\frac{1}{2}}, \tag{2}$$

where Θ is $\mathrm{N} \times \mathrm{N}$ matrix of cross-correlations between N transmit antennas. Similarly, Φ is $\mathrm{M} \times \mathrm{M}$ matrix of cross-correlations between M receive antennas. All entries of the kernel $\widehat{\mathcal{H}}$ in (2) are assumed to be zero-mean, independent and identically distributed random variables.

Correlation between transmit antennas n' and n is a function of their separation in wavelengths, as $\Theta(n', n) = \mathrm{J}_0\left(2\pi \left|\left|r_{n'} - r_n\right|\right|/\lambda\right)$. Here, r_n is the three-dimensional position vector of n-th transmit antenna, λ is the carrier wavelength, and J_0 is the Bessel function of zeroth order. Reference origin for the position vector r_n of $n-$th antenna is irrelevant because separation between antennas n and n' is given as $||r_{n'} - r_n||$, which only depends on the relative antenna spacing.

Receive antenna correlation Φ is usually modeled analogous to Θ. However, we note that authors which consider dense multiantenna receivers [8, 11, 12] have often adopted passive[4] channel model, which is to set $\Phi(m', m) = \mathrm{M}^{-1}\mathrm{J}_0\left(2\pi \left|\left|r_{m'} - r_m\right|\right|/\lambda\right)$, to keep the average received power normalized to unity. We will make certain conclusions independently of the M^{-1} normalization, which is why we initially adopt a generic Φ. Conversely, conclusions which depend on the model normalization will be discussed separately.

Finally, the kernel $\widehat{\mathcal{H}}$ is assumed to be isotropically invariant random matrix. As a reminder, isotropically invariant random matrices are those whose probability distribution remains unchanged, when the matrix is pre or post-multiplied by any unitary matrix. Most common example is i.i.d. complex Gaussian, which models Rayleigh fading. Channel model (2) can be derived using ray-tracing methodology [6], with the assumption that both transmitter and receiver are located in well-scattered environments, where paths depart/arrive from all directions.

2.2 Spectral Efficiency at Low Powers

The achievable data rate R [bits]/[sec $\times$ Hz], of a point-to-point communication system, is commonly described as a function of the average power P [Joules]/[sec $\times$ Hz], which is consumed by the transmitter. Rather than explicitly using $R(P)$, recent discoveries in information theory [3, 7] provide a convenient mathematical framework for *the low power regime*, by suggesting an alternate representation for R.

In order to gauge the bandwidth requirement for a low power system, [3] shows that the key tradeoff is between R and aggregate transmitted energy per information bit $\mathcal{E} = P/R$. Following [3], we will distinguish between functions $R(P)$ and $R(\mathcal{E})$, where the function $R(\mathcal{E})$ is termed "spectral efficiency."

Under the mild assumption of finite received power, energy per information bit $\mathcal{E}$ remains bounded below [3]. The lower bound is commonly denoted as $\mathcal{E}_{\min}$, and low power systems are defined as systems which operate close to $\mathcal{E}_{\min}$. According to the convention which is established in [3] and used in [7], spectral efficiency is well approximated with

$$R(\mathcal{E}) = \mathcal{S}\left[\log_2 \mathcal{E} - \log_2 \mathcal{E}_{\min}\right] + \epsilon, \tag{3}$$

[4]In fact [12] considers "normalized capacity," which is mathematically equivalent to the capacity of the passive channel model.

where $\epsilon \to 0$ as $\mathcal{E} \to \mathcal{E}_{\min}$. Communication limits of low power systems are described by finding both $\mathcal{E}_{\min}$ and $\mathcal{S}$. Following Theorem [3] characterizes $\mathcal{E}_{\min}$ and $\mathcal{S}$ for channel (1).

Theorem 1 (Verdu [3]). *For Channel Model (1), we have*

$$\mathcal{E}_{\min} = \frac{\mathrm{N} \ln 2}{\operatorname{tr} \mathrm{E}\left[\mathcal{H}\mathcal{H}^{\dagger}\right]}, \tag{4}$$

where "tr" is the trace operator on a matrix. Furthermore, we have

$$\mathcal{S} = 2 \frac{\left[\operatorname{tr} \mathrm{E}\left[\mathcal{H}\mathcal{H}^{\dagger}\right]\right]^2}{\operatorname{tr} \mathrm{E}\left[\left[\mathcal{H}\mathcal{H}^{\dagger}\right]^2\right]}. \tag{5}$$

Benchmark special case of Theorem 1 is given for a deterministic single-antenna channel, where $\mathcal{H} = h$ is constant, and the slope $\mathcal{S}$ in (5) becomes 2. Fading environment reduces the spectral efficiency slope of single-antenna channels as $\mathcal{S} = 2\kappa^{-1}(h)$, where $\kappa(h)$ is the kurtosis of fading distribution on h. Kurtosis always satisfies $\kappa(h) \geq 1$, and it essentially captures the penalty which is incurred on spectral efficiency due to fading. In subsequent sections, we address communication limits of multi-antenna configurations, given only a constraint of bounded transceiver aperture.

3 Effective Degrees of Freedom

In this section, we introduce a new parameter: *the effective degrees of freedom* ω, which we use to characterize antenna configurations that operate in the low power regime. Effective degrees of freedom will help us address the practical problem of capacity-based antenna configuration design. Here, we will simply maximize spectral efficiency over transmit and receive antenna configurations, and show how ω naturally emerges as the most appropriate characterization of an antenna configuration.

The first step is to evaluate spectral efficiency for correlated antenna arrays. For this purpose, we start from Theorem 1 by computing averages in (4) and (5), where we model $\mathcal{H}$ as in (2). This outlines the proof of Theorem 2, which follows next, and whose special case ($\kappa = 2$) can be found in [7].

Theorem 2 (Correlated Arrays). *For channel model (1) and (2), we have*

$$\mathcal{E}_{\min} = \frac{\ln 2}{[\operatorname{tr} \Phi] \, \mathrm{E}\left[|\widehat{h}|^2\right]}, \tag{6}$$

where $\widehat{h}$ denotes a generic entry of the kernel matrix $\widehat{\mathcal{H}}$ from (2). Furthermore, we let κ denote the kurtosis of a $\widehat{h}$. Spectral efficiency slope satisfies

$$\frac{2}{\mathcal{S}} = \frac{\operatorname{tr}\left[\Phi^2\right] \operatorname{tr}\left[\Theta^2\right]}{\left[\operatorname{tr} \Phi\right]^2 \left[\operatorname{tr} \Theta\right]^2} [\kappa - 2] + \frac{\operatorname{tr}\left[\Phi^2\right]}{\left[\operatorname{tr} \Phi\right]^2} + \frac{\operatorname{tr}\left[\Theta^2\right]}{\left[\operatorname{tr} \Theta\right]^2}. \tag{7}$$

Proof. Major computations, which are required for the proof of this theorem, involve averages in the numerator and denominator of the expression (5) for the spectral efficiency slope. These computations are summarized in the following two Lemmas.

Lemma 1. *Let* $\mathcal{H} = \Phi^{\frac{1}{2}}\widehat{\mathcal{H}}\Theta^{\frac{1}{2}}$, *where* $\widehat{\mathcal{H}}$ *is zero-mean, isotropically invariant* $\mathrm{M} \times \mathrm{N}$ *matrix, with independent and identically distributed entries. Generic entry of* $\widehat{\mathcal{H}}$ *will be denoted as* $\widehat{h}$. *We claim that*

$$\mathrm{E}\left[\mathcal{H}\mathcal{H}^\dagger\right] = \Phi\,[\mathrm{tr}\,\Theta]\;\mathrm{E}\left[|\widehat{h}|^2\right]. \tag{8}$$

Lemma 2. *Under same conditions as in Lemma 1, we have*

$$\begin{aligned}\mathrm{E}\,\mathrm{tr}\left[\left(\mathcal{H}\mathcal{H}^\dagger\right)^2\right] &= \mathrm{tr}\left[\Phi^2\right]\;\mathrm{tr}\left[\Theta^2\right]\left[\mathrm{E}\left[|\widehat{h}|^4\right] - 2\,\mathrm{E}\left[|\widehat{h}|^2\right]^2\right] + \\ &+ \left[\mathrm{tr}\left[\Theta^2\right][\mathrm{tr}\,\Phi]^2 + \mathrm{tr}\left[\Phi^2\right][\mathrm{tr}\,\Theta]^2\right]\mathrm{E}\left[|\widehat{h}|^2\right]^2.\end{aligned} \tag{9}$$

Proofs for both Lemmas 1 and 2 are found in Appendices A and B, respectively.

Using Lemma 1, along with (4) from Theorem 1, we conclude that

$$\mathcal{E}_{\min} = \frac{\mathrm{N}\ln 2}{\mathrm{tr}\,\mathrm{E}\left[\mathcal{H}\mathcal{H}^\dagger\right]} = \frac{\mathrm{N}\ln 2}{\mathrm{tr}\,[\Phi]\,\mathrm{tr}[\Theta]\,\mathrm{E}\left[|\widehat{h}|^2\right]}. \tag{10}$$

Expression (10) is the same as (6), because $\mathrm{tr}[\Theta] = \mathrm{N}$. Finally, using Lemma 1 for the numerator in expression (5), together with the Lemma 2 for the denominator, we have

$$\begin{aligned}\frac{2}{\mathcal{S}} = \frac{\mathrm{tr}\,\mathrm{E}\left[\left[\mathcal{H}\mathcal{H}^\dagger\right]^2\right]}{\left[\mathrm{tr}\,\mathrm{E}\left[\mathcal{H}\mathcal{H}^\dagger\right]\right]^2} &= \frac{\mathrm{tr}\left[\Phi^2\right]\;\mathrm{tr}\left[\Theta^2\right]\left[\mathrm{E}\left[|\widehat{h}|^4\right] - 2\,\mathrm{E}\left[|\widehat{h}|^2\right]^2\right]}{\left[\mathrm{tr}\,[\Phi]\;\mathrm{tr}[\Theta]\,\mathrm{E}\left[|\widehat{h}|^2\right]\right]^2} + \\ &+ \frac{\left[\mathrm{tr}\left[\Theta^2\right][\mathrm{tr}\,\Phi]^2 + \mathrm{tr}\left[\Phi^2\right][\mathrm{tr}\,\Theta]^2\right]\mathrm{E}\left[|\widehat{h}|^2\right]^2}{\left[\mathrm{tr}\,[\Phi]\,\mathrm{tr}[\Theta]\;\mathrm{E}\left[|\widehat{h}|^2\right]\right]^2},\end{aligned} \tag{11}$$

which is the same as (7), and completes the proof of this Theorem. □

Using Theorem 2, we are able to effectively address the antenna array design problem, where we maximize the spectral efficiency (3), over various transmit and receive antenna configurations. Here, Theorem 2 provides parameters $(\mathcal{E}_{\min}, \mathcal{S})$ for the spectral efficiency approximation (3). By studying the effect of antenna correlation on $(\mathcal{E}_{\min}, \mathcal{S})$, we will be able to first describe, and then optimize the spectral efficiency (3), with respect to various antenna configurations.

From (6), we note that $\mathcal{E}_{\min}$ is independent from the number of transmit antennas and their configuration [3, 7]. For a fixed number of receive antennas, $\mathcal{E}_{\min}$ is also independent of the actual receiver configuration, because diagonal entries of Φ represent the average power gain for each receive antenna. If we adopt the passive channel model from [8, 11, 12] where $\Phi(m', m) = \mathrm{M}^{-1}\mathrm{J}_0\left(2\pi\,||r_{m'} - r_m||/\lambda\right)$, we have $\mathrm{tr}\,(\Phi) = 1$ and $\mathcal{E}_{\min}$ is independent from the number of receive antennas as well. In general, we conclude that actual antenna configurations have no impact on $\mathcal{E}_{\min}$, which is why we focus on those configurations which maximize $\mathcal{S}$.

From the expression for $\mathcal{S}$ in (7), we observe that the impact of receiver correlation Φ can be summarized by a single real number $\omega_{\mathrm{R}} \in \mathbb{R}^+$, which we introduce next.

Definition 1. Effective degrees of freedom *of the receiver are defined as*

$$\omega_{\mathrm{R}} \triangleq \frac{[\operatorname{tr} \Phi]^2}{\operatorname{tr}\left[\Phi^2\right]}. \tag{12}$$

Effective degrees of freedom of the transmitter array are labeled as ω_{T}, *and are defined analogous to (12), where* Φ *is replaced by* Θ.

Using definition (12), spectral efficiency slope (7) becomes

$$2\mathcal{S}^{-1} = \omega_{\mathrm{T}}^{-1}\omega_{\mathrm{R}}^{-1}(\kappa - 2) + \omega_{\mathrm{T}}^{-1} + \omega_{\mathrm{R}}^{-1}. \tag{13}$$

The nomenclature "effective degrees of freedom" is justified by considering (13) for the baseline case study of uncorrelated arrays, which is found in [3]. If transmit and receive arrays are uncorrelated then (13) becomes $2\mathcal{S}^{-1} = \mathrm{M}^{-1}\mathrm{N}^{-1}(\kappa-2)+\mathrm{M}^{-1}+\mathrm{N}^{-1}$, whereas in the presence of antenna correlation M generalizes to ω_{R}, and N generalizes to ω_{T}. Furthermore, ω_{R} does not depend on the channel gain, because it remains unaltered when Φ is scaled by any real number[5]. From (13), we also note that when $\omega_{\mathrm{T}} \to \infty$, then $\mathcal{S} = 2\,\omega_{\mathrm{R}}$, which is essentially ω_{R} multiple of spectral efficiency slope for AWGN channel. Hence, the spectral efficiency (3), which is achieved with the receive configuration Φ, is ω_{R} multiple of spectral efficiency for AWGN.

We will utilize the effective degrees of freedom ω_{R} and ω_{T} as a very convenient tool, for optimizing the growth (13) of spectral efficiency. Following properties of ω_{T} and ω_{R} are of interest.

Proposition 1 (Properties of ω). *The following holds:*

1. *When* ω_{R} *or* ω_{T} *increases, the spectral efficiency slope* $\mathcal{S}$ *increases as well.*

2. *Effective degrees of freedom of the transmitter are inversely proportional to the total squared transmit antenna correlation, like*

$$\omega_{\mathrm{T}} = \frac{\mathrm{N}^2}{\mathrm{TSC}_{\mathrm{T}}}, \tag{14}$$

   where $\mathrm{TSC}_{\mathrm{T}} = \sum_m \sum_{m'} [\Theta(m', m)]^2$ *and* Θ *is the transmit correlation matrix. Similarly, effective degrees of freedom of the receiver are inversely proportional to the total square receive antenna correlation.*

3. *For an arbitrary* $\mathrm{M} \times \mathrm{M}$ *receive correlation matrix* Φ, *it holds* $1 \leq \omega_{\mathrm{R}} \leq \mathrm{M}$. *Upper bound is reached for uncorrelated array where* $\omega_{\mathrm{R}} = \mathrm{M}$. *Lower bound is reached for a perfectly correlated, i.e., phased array, where all entries of* Φ *are equal and* $\omega_{\mathrm{R}} = 1$. *Similarly,* $1 \leq \omega_{\mathrm{T}} \leq \mathrm{N}$.

Proof. 1. To prove that $\mathcal{S}$ increases as ω_{R} increases, it suffices to show that $\mathcal{S}^{-1}$ decreases when ω_{R}^{-1} decreases. Equivalently, we will show that derivative of $\mathcal{S}^{-1}$, taken with respect to ω_{R}^{-1} is non-negative. We have that

$$2\,\frac{\mathrm{d}\left[\mathcal{S}^{-1}\right]}{\mathrm{d}\left[\omega_{\mathrm{R}}^{-1}\right]} = \omega_{\mathrm{T}}^{-1}(\kappa - 1) \geq 0, \tag{15}$$

[5]This also implies that ω_{R} remains the same whether or not we adopt the correlation model $\Phi(m', m) = \mathrm{M}^{-1}\mathrm{J}_0\left(2\pi\,||r_{m'} - r_m||/\lambda\right)$ in [8, 11, 12].

because fading kurtosis always satisfies $\kappa \geq 1$, and because $\omega_{\mathrm{T}} \geq 0$. Therefore, $\mathcal{S}$ increases when ω_{R} increases. By symmetry of ω_{T} and ω_{R} in (13), $\mathcal{S}$ also increases when ω_{T} grows.

2. Follows directly from computing the numerator and denominator in the definition of effective degrees of freedom.

3. The last part claims upper and lower bounds on ω_{R}, as $1 \leq \omega_{\mathrm{R}} \leq \mathrm{M}$. First we focus on the upper bound $\omega_{\mathrm{R}} \leq \mathrm{M}$, which is by definition (13) equivalent to $(\mathrm{tr}\ \Phi)^2 \leq \mathrm{M}\,\mathrm{tr}\left(\Phi^2\right)$. The proof will consist of two steps, and the first step is to consider only diagonal Φ.

Notice that $(\mathrm{tr}\ \Phi)^2$ can be written as

$$\left[\sum_{m=1}^{\mathrm{M}} \Phi(m,m)\right]^2 = \sum_{m=1}^{\mathrm{M}} \sum_{m'=1}^{\mathrm{M}} \Phi(m,m)\Phi(m',m') \tag{16}$$

$$\leq \sum_{m=1}^{\mathrm{M}} \sum_{m'=1}^{\mathrm{M}} \frac{1}{2}\left[[\Phi(m,m)]^2 + [\Phi(m',m')]^2\right] = \mathrm{M}\sum_{m=1}^{\mathrm{M}} [\Phi(m,m)]^2 . \tag{17}$$

The right hand side of (17) is $\mathrm{M}\,\mathrm{tr}\left(\Phi^2\right)$ because Φ is assumed to be diagonal. This completes the proof of $(\mathrm{tr}\ \Phi)^2 \leq \mathrm{M}\,\mathrm{tr}\left(\Phi^2\right)$ for the case of diagonal Φ. Note that in transition from (16) to (17) we used the simple fact that $2\Phi(m,m)\Phi(m',m') \leq [\Phi(m,m)]^2 + [\Phi(m',m')]^2$, which is equivalent with an obvious inequality $[\Phi(m,m) - \Phi(m',m')]^2 \geq 0$.

By adding off-diagonal entries to Φ, then $\mathrm{tr}\left(\Phi^2\right) = \|\Phi\|_{\mathrm{FRO}}^2$ only grows because Φ is symmetric ("FRO" denotes a Frobenius norm of a matrix). While $\mathrm{tr}\left(\Phi^2\right)$ only grows from adding off-diagonal elements, the left hand side $(\mathrm{tr}\ \Phi)^2$ stays the same irrespective of non-diagonal entries, which means that inequality $(\mathrm{tr}\ \Phi)^2 \leq \mathrm{M}\,\mathrm{tr}\left(\Phi^2\right)$ only becomes stronger when Φ is non-diagonal. This completes the second step. From (17), the equality condition $(\mathrm{tr}\ \Phi)^2 = \mathrm{M}\,\mathrm{tr}\left(\Phi^2\right)$ holds if and only if Φ is exactly diagonal and all $\Phi(m,m)$ are equal, which is the case of perfectly uncorrelated antennas.

Finally, we prove the lower bound $1 \leq \omega_{\mathrm{R}}$, which is equivalent to $(\mathrm{tr}\ \Phi)^2 \geq \mathrm{tr}\left(\Phi^2\right)$. For that purpose, we let $\Phi = Q\Lambda Q^\dagger$ be the eigenvalue decomposition of Φ. We have that $\mathrm{tr}\ \Phi = \mathrm{tr}\ \Lambda$, and that $\mathrm{tr}\left(\Phi^2\right) = \mathrm{tr}\left(Q\Lambda Q^\dagger Q\Lambda Q^\dagger\right) = \mathrm{tr}\left(\Lambda^2\right)$. Hence, all we need to show is that $(\mathrm{tr}\ \Lambda)^2 \geq \mathrm{tr}\left(\Lambda^2\right)$ for the diagonal matrix of eigenvalues. The last inequity is obvious, because $(\mathrm{tr}\ \Lambda)^2$ is square of a sum, while $\mathrm{tr}\left(\Lambda^2\right)$ is sum of squares. To conclude, we observe that equality holds in $(\mathrm{tr}\ \Phi)^2 \geq \mathrm{tr}\left(\Phi^2\right)$ if and only if Φ has only one non-zero eigenvalue, which occurs only when all antennas are perfectly correlated. □

In order to provide more intuition about appropriate antenna positioning, it is instructive to consider the following two examples, which highlight the impact of antenna correlation and separation on the effective degrees of freedom.

Example 1 (Two Element Array). Consider a very simple transmit antenna array, with only two elements, separated by a distance d. Correlation matrix of the array is

$$\Theta = \begin{bmatrix} 1 & \mathrm{J}_0\left(2\pi\frac{\mathrm{d}}{\lambda}\right) \\ \mathrm{J}_0\left(2\pi\frac{\mathrm{d}}{\lambda}\right) & 1 \end{bmatrix}, \tag{18}$$

which means that $[\mathrm{tr}\,\Theta]^2 = 4$ and also $\mathrm{tr}[\Theta^2] = 2 + 2\,\mathrm{J}_0^2\left(2\pi\frac{\mathrm{d}}{\lambda}\right)$.

Effective degrees of freedom parameter for the array is calculated as

$$\omega_{\mathrm{T}} = \frac{2}{1 + \mathrm{J}_0^2\left(2\pi\frac{\mathrm{d}}{\lambda}\right)}. \tag{19}$$

As antenna separation d ranges from 0 to λ, effective degrees of freedom range between 1 and 2. However, the relationship between ω_{T} and antenna separation d is non-monotonic, which is illustrated in Figure 1; hence, increasing d is not always beneficial. Namely, taking $\omega_{\mathrm{R}} = 2$ for the sake of comparison, the slope of spectral efficiency becomes

$$S_{2\times 1} = \frac{2}{1 + \frac{1}{2}\mathrm{J}_0^2\left(2\pi\frac{\mathrm{d}}{\lambda}\right) + \frac{1}{4}(\kappa - 2)\left[1 + \mathrm{J}_0^2\left(2\pi\frac{\mathrm{d}}{\lambda}\right)\right]},$$

which is also illustrated in Figure 1, for the case of Rayleigh fading where $\kappa = 2$. Following the same trend as ω_{T}, the slope of spectral efficiency is non-monotonic in antenna separation d.

Fortunately, Figure 1 also demonstrates existence of separation d for which the transmitter has full two effective degrees of freedom. This separation can be found from $2\pi\frac{\mathrm{d}}{\lambda} = 2.404$, which is the first zero of the Bessel function J_0. However, this principle cannot be generalized for arrays with more than two antennas, because zeros of the Bessel function are not uniformly spaced [13].

Example 2 (Three Element Linear Array). Consider a three-element (say transmit) linear array, with first element fixed at location $x = 0$, second element positioned at $x = \mathrm{d}$ and the third element fixed at $x = \mathrm{d}_1$. Elements are arranged in a straight line, where $\mathrm{d}_1 \geq \mathrm{d} \geq 0$. Correlation matrix of the array is therefore given as

$$\Theta = \left[\begin{array}{ccc} 1 & \mathrm{J}_0\left(2\pi\frac{\mathrm{d}}{\lambda}\right) & \mathrm{J}_0\left(2\pi\frac{\mathrm{d}_1}{\lambda}\right) \\ \mathrm{J}_0\left(2\pi\frac{\mathrm{d}}{\lambda}\right) & 1 & \mathrm{J}_0\left(2\pi\frac{\mathrm{d}_1-\mathrm{d}}{\lambda}\right) \\ \mathrm{J}_0\left(2\pi\frac{\mathrm{d}_1}{\lambda}\right) & \mathrm{J}_0\left(2\pi\frac{\mathrm{d}_1-\mathrm{d}}{\lambda}\right) & 1 \end{array}\right], \tag{20}$$

which means that effective degrees of freedom satisfy

$$\omega_{\mathrm{T}} = \frac{3^2}{3 + 2\left[\mathrm{J}_0^2\left(2\pi\frac{\mathrm{d}}{\lambda}\right) + \mathrm{J}_0^2\left(2\pi\frac{\mathrm{d}_1}{\lambda}\right) + \mathrm{J}_0^2\left(2\pi\frac{\mathrm{d}_1-\mathrm{d}}{\lambda}\right)\right]}. \tag{21}$$

Relationship (21) between effective d.o.f and the antenna placement is not straightforward, which in turn means that finding antenna configurations that maximize ω_{T} is non-trivial. Typical relation between effective d.o.f. and the array configuration is shown in Figure 2 for the smaller array ($\mathrm{d}_1 = \lambda$), and Figure 3 for the larger array ($\mathrm{d}_1 = 5\lambda$). As location of the second antenna ranges from one extreme point to another ($\mathrm{d}_1 \geq \mathrm{d} \geq 0$), the effective d.o.f function (21) *is not* maximized at the mid-point. In addition, we observe the symmetry of ω_{T} in Figures 2 and 3, which can be derived from substituting $\mathrm{d}_1 - \mathrm{d}$ for d in (21).

To conclude, uniformly spaced arrays are usually not optimal in terms of spectral efficiency. While deviation of uniform arrays from the optimum may appear small for an array of few elements - such as in Figure 2, as the number of elements in the array starts to grow, the deviation will increase (for some cases). In Section 5, we will present a method and several examples of construction of non-uniform arrays, which offer more than 30% gains over uniform arrays, in terms of spectral efficiency. □

Remark 1: Three clearly distinct phenomenon determine the growth (13) of spectral efficiency: effective d.o.f. at the transmitted, effective d.o.f. at the receiver and finally nature of the fading distribution, through the kurtosis κ. As fading kurtosis κ grows, the spectral efficiency reduces because $\frac{\mathrm{d}\mathcal{S}^{-1}}{\mathrm{d}\kappa} = \omega_{\mathrm{R}}^{-1}\omega_{\mathrm{T}}^{-1} > 0$. Indeed, for small ω_{R} and ω_{T}, the term $\omega_{\mathrm{R}}^{-1}\omega_{\mathrm{T}}^{-1}(\kappa-2)$ from (13) significantly impedes the growth of spectral efficiency.

On the other hand, when either ω_{T} or ω_{R} begins to increase, the fading distribution is rendered irrelevant, because $\omega_{\mathrm{R}}^{-1}\omega_{\mathrm{T}}^{-1}(\kappa-2) \ll \omega_{\mathrm{R}}^{-1}$ for $\omega_{\mathrm{T}} \to \infty$. In such case, the term $\omega_{\mathrm{R}}^{-1}\omega_{\mathrm{T}}^{-1}(\kappa-2)$ in (13) becomes insignificant. To conclude, in a system where effective d.o.f. of the transmitter or the receiver (or both) are large, the fading distribution has no real impact on the growth of spectral efficiency, which in turn becomes $\mathcal{S} = \frac{2\omega_{\mathrm{R}}\omega_{\mathrm{T}}}{\omega_{\mathrm{R}}+\omega_{\mathrm{T}}}$. Similar observation regarding the significance of the fading distribution was also made in [3], but only for a fully uncorrelated array.

Remark 2: As indicated in part 2 of Proposition 1, effective degrees of freedom grow by reducing the total squared correlation between antennas. It is worthwhile noting that the problem of signature sequence design, which was initiated by [18] in a different context, also targets minimizing total square correlation (TSC), only between signature sequences. In signature set design, the objective is to construct N sequences of length L symbols each, while obtaining minimum TSC. The well-known Welch bound [18] states that in order to construct N sequences with total square correlation TSC, it takes at least $\frac{\mathrm{N}^2}{\mathrm{TSC}}$ temporal degrees of freedom, namely $\frac{\mathrm{N}^2}{\mathrm{TSC}} \leq \mathrm{L}$.

Remarkably, Definition (12), which is the same as part 2 of Proposition 1, can be regarded as using the Welch lower bound $\frac{\mathrm{N}^2}{\mathrm{TSC}}$ to extrapolate degrees of freedom from a given antenna array. Namely, Definition (12) simply states that N antennas with TSC contain $\frac{\mathrm{N}^2}{\mathrm{TSC}}$ *effective* degrees of freedom. This analogy suggests an open question: is there a one-to-one correspondence between N antenna locations and N spreading sequences, both sharing the same cross-correlation matrix? Potential benefits of an affirmative answer are substantial, because extensive literature on sequence design would immediately become available for configuration design.

Remark 3: By maximizing the effective degrees of freedom (ω_{T} and ω_{R}), perfectly uncorrelated transmit and receive antenna arrays also maximize the spectral efficiency slope $\mathcal{S}$. Unfortunately, design of uncorrelated arrays in a limited and small transceiver volume is often impossible, which is why spectral efficiency has to be maximized using correlated arrays. By Proposition 1, maximization of $\mathcal{S}$ over a pair $(\omega_{\mathrm{T}}, \omega_{\mathrm{R}})$ simply decouples into individual maximization of ω_{T} and ω_{R}. Practical significance of this remark is that transmitter and receiver can be designed independently of each other, and still jointly optimize the communication system.

Remark 4: Finally, it is important to note that effective degrees of freedom (12) only depend on the array geometry, and that changing the index (T or R), which indicates the change in communication direction, does not change the effective degrees of freedom of an array. In other words, a given antenna array contains certain degrees of freedom, regardless of whether it is used for transmission or for reception. For this reason, the rest of the manuscript deals with a wireless transceiver which maximizes an ω, be it ω_{T} or ω_{R}. Next section introduces a theoretical benchmark for this maximization.

4 Limiting Degrees of Freedom

Dense multi-antenna transceivers [1, 10, 12] contain plenty of antenna elements, which are tightly packed inside a given volume $G \subseteq \mathbb{R}^3$. With many antennas, the number of possible antenna placements and the resulting design choices grow quickly. From the practical design point of view, we will be interested in how close to optimal is any given array configuration. To address this question, we introduce the following notion of *limiting degrees of freedom*, which we define as the least upper bound for effective degrees of freedom.

Definition 2. *For given aperture $G \subseteq \mathbb{R}^3$, we define* **limiting degrees of freedom** *as*

$$\Omega(G) \triangleq \sup_{\substack{|A|<\infty \\ A\subseteq G}} \frac{\left[\operatorname{tr} \Phi_A\right]^2}{\operatorname{tr}\left[\Phi_A^2\right]}. \tag{22}$$

Supremum (22) is taken over all possible configurations of finite number $|A| < \infty$ of antennas inside G, namely $A \subseteq G$. In (22), Φ_A denotes the correlation between antennas which are placed inside the finite set of discrete points A.

The notion of limiting degrees of freedom establishes a theoretical benchmark for effective degrees of freedom, by allowing arbitrary finite number of antennas $|A|$, in an arbitrary configuration Φ_A. Note that definition of limiting degrees of freedom (22) is applicable to both receive and transmit antenna arrays, where for the transmit antenna array Φ_A is replaced by Θ_A in (22).

For any antenna configuration A, correlation matrix Φ_A depends only on the ratio of antenna spacing to λ, which means that limiting degrees of freedom $\Omega(G)$ depend only on the size and shape of G with respect to the carrier wavelength λ. For example, doubling the choice of carrier frequency allows us to shrink the geometry G by a factor of two, and still maintain the same limiting degrees of freedom.

4.1 Basic Properties

Given an arbitrary transceiver aperture G, it is feasible to either compute $\Omega(G)$ in a closed form, or alternatively, to find $\Omega(G)$ numerically, by performing a search over antenna configurations. These two approaches will be covered in Sections 4.2 and 5 below. The main result of this section states that $\Omega(G)$ is finite for any bounded G; in other words, a bounded geometry can warrant only a finite number of degrees of freedom. Finiteness of $\Omega(G)$ is intuitive and practically important, since it will permit us to approach the limiting d.o.f. with a finite number of antennas for practical designs. To prove that $\Omega(G)$ is finite, we will first require the following three Properties (1-3).

Property 1. *Limiting degrees of freedom function $\Omega(G)$ is a monotonically non-decreasing set function. Specifically, if $G_1 \subseteq G_2$, then $\Omega(G_1) \leq \Omega(G_2)$.*

Property 2. *For a non-empty set $G \subseteq \mathbb{R}^3$, we have $\Omega(G) \geq 1$.*

Proofs of Properties 1 and 2 are simple observations. Property 1 is true because supremum (22) over a superset G_2 cannot be smaller. Property 2 is true because positioning a single antenna inside G results in the effective degrees of freedom of one. Less obvious but quite intuitive Property of limiting degrees of freedom is finite subadditivity, which is stated next.

Property 3. *Limiting degrees of freedom function is finitely sub-additive,*

$$\Omega\left(G_1 \cup G_2\right) \leq \Omega(G_1) + \Omega(G_2). \tag{23}$$

Proof. First, we require the following Lemma.

Lemma 3. *Let $A_1 \subseteq G_1$ and $A_2 \subseteq G_2$, where both A_1 and A_2 are finite antenna configurations. Let Φ_{A_1} denote the correlation matrix for points in A_1, and let Φ_{A_2} denote the correlation matrix for points in A_2. Finally, let Φ_{A_1,A_2} denote the cross-correlation between points from A_1 and points from A_2. Then*

$$\frac{\left(\operatorname{tr}\left[\Phi_{A_1}\right] + \operatorname{tr}\left[\Phi_{A_2}\right]\right)^2}{\operatorname{tr}\begin{bmatrix} \Phi_{A_1} & \Phi_{A_1,A_2} \\ \Phi_{A_2,A_1} & \Phi_{A_2} \end{bmatrix}^2} \leq \frac{\left[\operatorname{tr}\Phi_{A_1}\right]^2}{\operatorname{tr}\left[\Phi_{A_1}^2\right]} + \frac{\left[\operatorname{tr}\Phi_{A_2}\right]^2}{\operatorname{tr}\left[\Phi_{A_2}^2\right]}. \tag{24}$$

Proof. Note that (24) is equivalent to

$$\frac{\left(\operatorname{tr}\left[\Phi_{A_1}\right] + \operatorname{tr}\left[\Phi_{A_2}\right]\right)^2}{\operatorname{tr}\left[\Phi_{A_1}^2\right] + \operatorname{tr}\left[\Phi_{A_2}^2\right] + \operatorname{tr}\left[\Phi_{A_1,A_2}\Phi_{A_2,A_1}\right] + \operatorname{tr}\left[\Phi_{A_2,A_1}\Phi_{A_1,A_2}\right]} \leq \frac{\left[\operatorname{tr}\Phi_{A_1}\right]^2}{\operatorname{tr}\left[\Phi_{A_1}^2\right]} + \frac{\left[\operatorname{tr}\Phi_{A_2}\right]^2}{\operatorname{tr}\left[\Phi_{A_2}^2\right]}. \tag{25}$$

By the symmetry property of the cross-correlation matrix Φ, we have that $\Phi_{A_2,A_1} = \Phi^{\dagger}_{A_1,A_2}$. From here it follows that $\operatorname{tr}[\Phi_{A_1,A_2}\Phi_{A_2,A_1}] = \operatorname{tr}[\Phi_{A_1,A_2}\Phi^{\dagger}_{A_1,A_2}] = \|\Phi_{A_1,A_2}\|^2_{\text{FRO}} \geq 0$. Similarly, it also holds that $\operatorname{tr}\left[\Phi_{A_2,A_1}\Phi_{A_1,A_2}\right] \geq 0$. Therefore, the left hand side of (25) increases when we remove terms $\operatorname{tr}\left[\Phi_{A_2,A_1}\Phi_{A_1,A_2}\right]$ and $\operatorname{tr}\left[\Phi_{A_1,A_2}\Phi_{A_2,A_1}\right]$ from the denominator. Hence, to prove (25) it will suffice to show that

$$\frac{\left(\operatorname{tr}\left[\Phi_{A_1}\right] + \operatorname{tr}\left[\Phi_{A_2}\right]\right)^2}{\operatorname{tr}\left[\Phi_{A_1}^2\right] + \operatorname{tr}\left[\Phi_{A_2}^2\right]} \leq \frac{\left[\operatorname{tr}\Phi_{A_1}\right]^2}{\operatorname{tr}\left[\Phi_{A_1}^2\right]} + \frac{\left[\operatorname{tr}\Phi_{A_2}\right]^2}{\operatorname{tr}\left[\Phi_{A_2}^2\right]}, \tag{26}$$

because the left hand side of (26) is always greater than the left hand side of (25). Upon multiplication of (26) by the three denominators $\left[\operatorname{tr}\left[\Phi_{A_1}^2\right] + \operatorname{tr}\left[\Phi_{A_2}^2\right]\right] \operatorname{tr}\left[\Phi_{A_1}^2\right] \operatorname{tr}\left[\Phi_{A_2}^2\right]$ and canceling common terms, it reduces to the following

$$2\operatorname{tr}\left[\Phi_{A_1}\right]\operatorname{tr}\left[\Phi_{A_2}\right]\operatorname{tr}\left[\Phi_{A_1}^2\right]\operatorname{tr}\left[\Phi_{A_2}^2\right] \leq \left[\operatorname{tr}\Phi_{A_1}\right]^2\left(\operatorname{tr}\left[\Phi_{A_1}^2\right]\right)^2 + \left[\operatorname{tr}\Phi_{A_2}\right]^2\left(\operatorname{tr}\left[\Phi_{A_2}^2\right]\right)^2 \tag{27}$$

$$0 \leq \left(\operatorname{tr}\left[\Phi_{A_1}\right]\operatorname{tr}\left[\Phi_{A_2}^2\right] - \operatorname{tr}\left[\Phi_{A_2}\right]\operatorname{tr}\left[\Phi_{A_1}^2\right]\right)^2, \tag{28}$$

which completes the proof of this Lemma. □

Using the main statement (24) of Lemma 3, we have that

$$\frac{\left(\operatorname{tr}\left[\Phi_{A_1}\right] + \operatorname{tr}\left[\Phi_{A_2}\right]\right)^2}{\operatorname{tr}\begin{bmatrix} \Phi_{A_1} & \Phi_{A_1,A_2} \\ \Phi_{A_2,A_1} & \Phi_{A_2} \end{bmatrix}^2} \leq \sup_{\substack{A_1 \subseteq G_1 \\ |A_1| < \infty}} \frac{\left[\operatorname{tr}\Phi_{A_1}\right]^2}{\operatorname{tr}\left[\Phi_{A_1}^2\right]} + \sup_{\substack{A_2 \subseteq G_2 \\ |A_2| < \infty}} \frac{\left[\operatorname{tr}\Phi_{A_2}\right]^2}{\operatorname{tr}\left[\Phi_{A_2}^2\right]} \tag{29}$$

$$= \Omega(G_1) + \Omega(G_2). \tag{30}$$

To complete the last step of the proof for Property 2, we take the supremum on the left of (29), to arrive at $\Omega(G) \leq \Omega(G_1) + \Omega(G_2)$.

Examination of (25), (26) and (28) will produce necessary and sufficient condition for achieving the upper bound (23). Left hand sides of (25) and (26) are equal if and only if $\text{tr}(\Phi_{A_1,A_2}\Phi^{\dagger}_{A_1,A_2}) = \|\Phi_{A_1,A_2}\|^2_{\text{FRO}} = 0$, which means that each point of A_1 is fully uncorrelated with each point of A_2. As an approximation, this occurs when A_1 and A_2 are separated by several wavelengths, which is true when G_1 and G_2 are separated by several wavelengths. The equality in (28) is satisfied when $\text{tr}\left(\Phi_{A_1}\right)\text{tr}\left(\Phi^2_{A_2}\right) = \text{tr}\left(\Phi_{A_2}\right)\text{tr}\left(\Phi^2_{A_1}\right)$. To conclude, given G_1 and G_2 which are separated by several wavelengths, the upper bound (23) can only be achieved by designing configurations so that $\text{tr}\left(\Phi_{A_1}\right)\text{tr}\left(\Phi^2_{A_2}\right) = \text{tr}\left(\Phi_{A_2}\right)\text{tr}\left(\Phi^2_{A_1}\right)$. □

The utility of Property 2 is twofold. First, we will use it as a building block to prove finiteness of ω for any bounded aperture G. Second, when apertures G_1 and G_2 are very far apart, so that each point of G_1 is practically uncorrelated with each point of G_2, then (23) is becomes equality. In that case, we simply evaluate the individual limiting degrees of freedom for G_1 and G_2 separately to obtain $\Omega(G_1 \cup G_2)$.

Property 4. *For a bounded set G, the limiting degrees of function is finite.*

Proof. The result will be proved in two steps for clarity of exposition. In the first step, we address the scenario where space G has a certain size limitation (see below); in the second step, we generalize the proof for an arbitrary sized G.

Step 1. Choose any $\epsilon \in (0, 1)$. Let a be the smallest non-negative real number, for which it holds that $\text{J}_0\left(2\pi\left[\frac{a}{\lambda}\right]\right) > \epsilon$. Since the Bessel function is monotonically decreasing before the first zero, then $\text{J}_0\left(2\pi\left[\frac{x}{\lambda}\right]\right) > \text{J}_0\left(2\pi\left[\frac{a}{\lambda}\right]\right)$ for $x \in (0, a)$. Now, suppose that space G is small enough to be covered by a sphere of diameter a. If A is any finite subset of G, then each individual entry of the correlation matrix Φ_A is greater than ϵ, because of the condition that $\text{J}_0\left(2\pi\left[\frac{x}{\lambda}\right]\right) > \text{J}_0\left(2\pi\left[\frac{a}{\lambda}\right]\right) > \epsilon$. Noting $\text{tr}\left(\Phi^2_A\right) = \|\Phi_A\|^2_{\text{FRO}} \geq \epsilon^2|A|^2 = \epsilon^2\,\text{tr}\left(\Phi_A\right)^2$, where $|A|$ is the cardinality of A, it follows that

$$\frac{\left[\text{tr}\,\Phi_A\right]^2}{\text{tr}\left[\Phi^2_A\right]} \leq \epsilon^{-2} < \infty. \tag{31}$$

Since (31) is true for an arbitrary configuration A, and ϵ is independent from the configuration, taking the supremum over all $A \subseteq G$ and $A < \infty$ on the left hand side of (31) results in $\Omega(G) \leq \epsilon^{-2} < \infty$. This completes the Step 1.

Step 2. Here, we address the case of arbitrary sized G. Main idea is reduction to Step 1, and the use of monotonicity (Property 1) and subadditivity (Property 3) of limiting degrees of freedom. Given any bounded aperture G, it can be covered by finitely many G_k, where G_k are spheres with diameter a, as specified in the Step 1. We therefore have $G \subseteq \bigcup_{\text{k}=1}^{K} G_\text{k}$. From here, we first use the monotonicity, and then the finite subadditivity to arrive at

$$\Omega(G) \leq \Omega\left(\bigcup_{\text{k}=1}^{K} G_\text{k}\right) \leq \sum_{\text{k}=1}^{K}\Omega(G_\text{k}) \leq K\epsilon^{-2} < \infty. \tag{32}$$

This completes the proof of Property 4, for an arbitrary shaped G. □

Property 4 claims that no antenna packing inside a bounded space G will yield infinite effective degrees of freedom ω. Hence, in order to exploit spectral efficiency gains which are linearly proportional to the increasing number of antennas, the transceiver volume G must increase unboundedly. Because ω exhibits the saturation effect due to finiteness of G, so does the spectral efficiency from (13). Namely, even with an infinite number of antennas which are packed inside G, the spectral efficiency will still be finite. We next provide a concrete example of this phenomenon, where we evaluate the limiting degrees of freedom for a circular array.

4.2 Limiting Degrees of Freedom of Circular Array

When computing limiting degrees of freedom for a circle, we are faced with a very peculiar phenomenon that uniform circular arrays are not necessarily optimum antenna configurations. For example, consider placing $\mathrm{M} = 2$ antennas on a circle whose radius satisfies $\mathrm{J}_0\left(2\pi\left[\frac{2r}{\lambda}\right]\right) \neq 0$ and $2\pi\left[\frac{2r}{\lambda}\right] \geq 2.404$, where 2.404 is the first zero of the Bessel function. Here, positioning two antennas diametrically opposite is strictly suboptimum, because they will be correlated. Superior configuration is the one for which distance between antenna locations corresponds to the first zero of J_0, which produces an array of two perfectly uncorrelated antennas.

This phenomenon is also reflected in Figure 4, which depicts effective degrees of freedom ω versus the number of antennas that are uniformly located on the circle. Curve labeled as $r = \lambda$ in Figure 4 is not monotonically increasing, which means that increasing number of uniform antennas on the circle can actually reduce ω. In particular, by migrating from the uniform circular array of $\mathrm{M} = 8$ antennas towards the uniform circular array of $\mathrm{M} = 10$ antennas, ω reduces from $\omega = 7$ to $\omega = 6$. When these antennas transmit independent streams of data, the spectral efficiency actually reduces by increasing the number of antennas! The same conclusion holds for the receive mode, when we adopt the passive channel model from [8, 11, 12], where aggregate receive power is kept constant.

We compute the limiting d.o.f. of circular array in Theorem 3 below. The proof of Theorem 3 also shows why uniform antenna configuration on a circle becomes near-optimum in the limit as $\mathrm{M} \to \infty$.

Theorem 3. *If G is a circle of radius r, and if the carrier wavelength is λ, then*

$$\Omega^{-1}(G) = \frac{1}{2\pi}\int_{-\pi}^{\pi}\left|\mathrm{J}_0\left(\frac{2\pi r}{\lambda}\sqrt{2-2\cos\varphi}\right)\right|^2 d\varphi. \tag{33}$$

Proof. The goal is to prove that $\Omega(G)$ from (33) is the least upper bound for the effective degrees of freedom of an *arbitrary* circular configuration. For simplicity, we present the proof in two steps. In the first step, we focus on configurations that are constrained to angle values of φ which are rational multiples of 2π. In the second step, we extend the proof for arbitrary circular configurations.

<u>Step 1.</u> Consider an arbitrary finite antenna configuration A_1, with the constraint that antennas are located on angle values of φ which are rational multiples of 2π. Let A_2 be a uniform finite antenna configuration which is superset of the original one, namely $A_1 \subset A_2$, like illustrated in the Figure 5. The finite configuration A_2 which is portrayed on the second circle in Figure 5, exists only because of the initial constraint that A_1 is located on rational multiples of 2π. We next show that A_2 renders more effective degrees of freedom than A_1.

To demonstrate this, we will first show and then utilize the following simple inequality

$$\omega_{A_1}^{-1} = \frac{\operatorname{tr}\left[\Phi_{A_1}^2\right]}{\left[\operatorname{tr}\Phi_{A_1}\right]^2} = \frac{\operatorname{tr}\left[\Phi_{A_1}^2\right]}{|A_1|^2} \geq \min_{p^{\mathrm{T}}\mathbf{1}=1} p^{\mathrm{T}}\left[\Phi_{A_2} \odot \Phi_{A_2}^{\dagger}\right] p, \tag{34}$$

where $\odot$ is the elementwise (Hadamard) product of two equal sized matrices. Note that entries of $\Phi_{A_2} \odot \Phi_{A_2}^{\dagger}$ are square antenna correlations for configuration A_2. Inequality in (34) is trivially true, because by putting $p_{A_1} = 1/|A_1|$ for indexes in A_1 and 0 otherwise on the right of (34) produces the left of (34). Since the right hand side of (34) is minimized over all choices for the vector p, it must be less or equal than the left side of (34).

To prove that antenna configuration A_2 offers more effective degrees of freedom than configuration A_1 (meaning that $\omega_{A_2} \geq \omega_{A_1}$), we show that the right hand side of (34) is in fact $\omega_{A_2}^{-1}$. This is the topic of the following lemma.

Lemma 4. *The right hand side of (34) equals*

$$\min_{p^{\mathrm{T}}\mathbf{1}=1} p^{\mathrm{T}}\left[\Phi_{A_2} \odot \Phi_{A_2}^{\dagger}\right] p = \frac{\operatorname{tr}\left[\Phi_{A_2}^2\right]}{\left[\operatorname{tr}\Phi_{A_2}\right]^2} = \omega_{A_2}^{-1}, \tag{35}$$

which is achieved only for $p = \left[\frac{1}{|A_2|}\right] \mathbf{1}$. *Here,* $\mathbf{1}$ *is the vector of all ones.*

Proof. The matrix $\Phi_{A_2} \odot \Phi_{A_2}^{\dagger}$ is non-negative, because it is a Hadamard product of two non-negative (correlation) matrices Φ_{A_2}. This fact is a direct consequence of the well-known Hadamard Product Lemma, whose proof is found in [16]. Since the matrix $\Phi_{A_2} \odot \Phi_{A_2}^{\dagger}$ is non-negative, then $p^{\mathrm{T}}\left[\Phi_{A_2} \odot \Phi_{A_2}^{\dagger}\right] p$ is convex ($\cup-$shaped) function of the vector p. Therefore, the Lagrange Multiplier strategy is guaranteed to produce the minimum (35). For this purpose, we let μ be the Lagrange multiplier for the constraint $p^{\mathrm{T}}\mathbf{1} = 1$. Lagrangian function is given in (36), its differential is set to zero in (37), and the solution for p is given in (38), as

$$p^{\mathrm{T}}\left[\Phi_{A_2} \odot \Phi_{A_2}^{\dagger}\right] p + \mu\left(p^{\mathrm{T}}\mathbf{1} - 1\right) \tag{36}$$

$$\left[\Phi_{A_2} \odot \Phi_{A_2}^{\dagger}\right] p = \mu\,\mathbf{1} \tag{37}$$

$$p = \mu\left[\Phi_{A_2} \odot \Phi_{A_2}^{\dagger}\right]^{-1} \mathbf{1}. \tag{38}$$

In transition from (36) to (37), which is done by differentiation, we used the abbreviated μ instead of -2μ, to reduce our calculations. In (38), the Lagrange multiplier μ must be the reciprocal of $\mathbf{1}^{\mathrm{T}}[\Phi_{A_2} \odot \Phi_{A_2}^{\dagger}]^{-1}\mathbf{1}$, because p must sum to unity.

Since A_2 is by construction uniform circular array, then $\Phi_{A_2} \odot \Phi_{A_2}^{\dagger}$ must be Toeplitz matrix, where each row is obtained from the previous one by a circular shift. All rows of $\Phi_{A_2} \odot \Phi_{A_2}^{\dagger}$ therefore sum equally, which means that $p = \frac{1}{|A_2|}\mathbf{1}$ satisfies (37) by inspection. This optimal choice of p produces the equality in (35) and completes the proof of this Lemma. □

Lemma 4 demonstrates that uniform circular array A_2 yields larger effective degrees of freedom from the original configuration A_1. Next, we simply continue the process with A_3 which is uniform circular array that contains A_2, and in general with A_{k} which contains

$A_{\mathrm{k}-1}$, as illustrated in the Figure 5. In order to obtain the limit point for the effective degrees of freedom when $\mathrm{k} \to \infty$, we first find $\mathrm{tr}\left[\Phi^2_{A_{\mathrm{k}}}\right]$ for a generic uniform circular array.

For a generic uniform circular array, the sum square correlation from the antenna which is located at $\varphi = 0$, to all antennas (including itself) is given as

$$\sum_{n=0}^{|A_{\mathrm{k}}|-1} \left| \mathrm{J}_0\left(\frac{2\pi r}{\lambda} \sqrt{2 - 2\cos\left[\frac{2\pi n}{|A_{\mathrm{k}}|}\right]} \right) \right|^2 \tag{39}$$

Justification for (39) is a simple cosine law: distance between two points on the circle of unit radius, which are φ apart is $2 - 2\cos(\varphi)$. For uniform circular array, we have $\varphi = \frac{2\pi n}{|A_{\mathrm{k}}|}$, and (39) follows. To obtain the total square correlation $\mathrm{tr}[\Phi^2_{A_{\mathrm{k}}}]$ between all points of the uniform circular array, we need to multiply (39) by the total number of antennas, which is $|A_{\mathrm{k}}|$.

Hence, we have that

$$\frac{\mathrm{tr}\left[\Phi^2_{A_{\mathrm{k}}}\right]}{\left[\mathrm{tr}\,\Phi_{A_{\mathrm{k}}}\right]^2} = \frac{\mathrm{tr}\left[\Phi^2_{A_{\mathrm{k}}}\right]}{|A_{\mathrm{k}}|^2} = \frac{1}{|A_{\mathrm{k}}|} \sum_{n=0}^{|A_{\mathrm{k}}|-1} \left| \mathrm{J}_0\left(\frac{2\pi r}{\lambda} \sqrt{2 - 2\cos\left[\frac{2\pi n}{|A_{\mathrm{k}}|}\right]} \right) \right|^2 \tag{40}$$

$$\downarrow \frac{1}{2\pi} \int_{-\pi}^{\pi} \left| \mathrm{J}_0\left(\frac{2\pi r}{\lambda} \sqrt{2 - 2\cos\varphi} \right) \right|^2 d\varphi. \tag{41}$$

Convergence in (41) is as $\mathrm{k} \to \infty$ and $A_{\mathrm{k}-1} \subset A_{\mathrm{k}}$, which is portrayed by the third circle in the Figure 5. Thus, beginning with an arbitrary antenna configuration A_1, which is located on rational multiples of 2π, we constructed the sequence A_{k} of antenna configurations, which monotonically increases effective degrees of freedom, to become the inverse of (41). This completes Step 1.

Step 2. In the last stage of the proof, we consider the case of initial configuration A, which is not located on rational multiples of 2π like A_1, and a finite uniformly spaced superset A_2 doesn't exist. Here, we invoke the continuity argument for the total square correlation, and for the function $[\mathrm{tr}\,\Phi_A]^2/\mathrm{tr}[\Phi^2_A]$, when A is finite. For brevity of exposition we label (41) as $\Omega^{-1}_{\mathrm{rat}}$.

Given any $\epsilon > 0$, and finite A which is located on the circle, there exists a finite A', which is located on rational multiples of 2π, close to A, and it holds that

$$\left| \frac{[\mathrm{tr}\,\Phi_A]^2}{\mathrm{tr}\left[\Phi^2_A\right]} - \frac{[\mathrm{tr}\,\Phi_{A'}]^2}{\mathrm{tr}\left[\Phi^2_{A'}\right]} \right| < \epsilon. \tag{42}$$

From the first stage of the proof, because A' is positioned on rational multiples of 2π, we have that $(\mathrm{tr}\,\Phi_{A'})^2/\mathrm{tr}(\Phi^2_{A'}) \leq \omega_{\mathrm{rat}}$. Combining this inequality with (42), we have that for any A,

$$\frac{[\mathrm{tr}\,\Phi_A]^2}{\mathrm{tr}\left[\Phi^2_A\right]} \leq \frac{[\mathrm{tr}\,\Phi_{A'}]^2}{\mathrm{tr}\left[\Phi^2_{A'}\right]} + \left| \frac{[\mathrm{tr}\,\Phi_A]^2}{\mathrm{tr}\left[\Phi^2_A\right]} - \frac{[\mathrm{tr}\,\Phi_{A'}]^2}{\mathrm{tr}\left[\Phi^2_{A'}\right]} \right| \leq \Omega_{\mathrm{rat}} + \epsilon. \tag{43}$$

Because ϵ is arbitrary small, we conclude that for any A, it holds $(\mathrm{tr}\,\Phi_A)^2/\mathrm{tr}(\Phi^2_A) \leq \Omega_{\mathrm{rat}}$. Hence, Ω_{rat}, which is the inverse of (41) is the least upper bound even for effective degrees of freedom, even for configurations which are not located on rational multiples of 2π. $\square$

Figure 4 illustrates the convergence of effective degrees of freedom towards the limiting degrees of freedom benchmark, for circles of various r/λ. For example, given a circle $r = \lambda$, limiting degrees of freedom function is approximately 11, which is closely achieved by a uniform circular array with only 14 antennas. Here, we conclude that 14 uniformly placed transmit antennas on a circle of $r = \lambda$ is a near-optimum configuration, and that positioning more antennas produces no effect on the spectral efficiency slope $\mathcal{S}$. If these antennas operate in the receive mode, and if we *do not* adopt the passive channel model from [8, 11, 12] then more antennas reduces $\mathcal{E}_{\min}$. In this case, we still conclude that for a fixed number of antennas beyond 14, uniform configuration is near-optimum.

Theorem 3 along with Figure 4 enables us to draw similar practical conclusions for other circular apertures. For example, 4 or more uniformly placed antennas is a near-optimum configuration for $r = 0.25\lambda$ and 8 or more uniformly positioned antennas is a near-optimum configuration for $r = 0.5\lambda$. Finally, for any given volume G_2, a simple lower bound for limiting d.o.f can be found by inscribing a smaller circle $G_1 \subseteq G_2$, and using the monotonicity of $\Omega(G)$.

4.2.1 Small-Sized Circular Arrays

Small-sized antenna arrays, whose diameter is on the order of centimeters, are gaining importance due to their portability and practicality for mobile applications [8, 12]. To address these, we next simplify the formula (33), under the assumption that r/λ is small.

Corollary 1. [to Theorem 3] *For small-sized circular arrays where $r/\lambda \to 0$, we have*

$$\Omega(G) = 1 + 4\pi^2 \left[\frac{r}{\lambda}\right]^2 + o\left(\left[\frac{r}{\lambda}\right]^2\right). \tag{44}$$

Proof. To prove (44), we will utilize the standard small-argument approximation for the Bessel function J_0. It can be found in [13] that

$$\mathrm{J}_0(z) = 1 - \frac{1}{4}z^2 + o\left(z^2\right) \;\Rightarrow\; |\mathrm{J}_0(z)|^2 = 1 - \frac{1}{2}z^2 + o\left(z^2\right). \tag{45}$$

Using (45), the limiting degrees of freedom expression (33) becomes

$$\Omega^{-1}(G) = \frac{1}{2\pi}\int_{-\pi}^{\pi} \left|\mathrm{J}_0\left(\frac{2\pi r}{\lambda}\sqrt{2 - 2\cos\varphi}\right)\right|^2 d\varphi \tag{46}$$

$$= \frac{1}{2\pi}\int_{-\pi}^{\pi} 1 - \frac{1}{2}\left[\frac{2\pi r}{\lambda}\right]^2 [2 - 2\cos\varphi] + o\left(\left[\frac{r}{\lambda}\right]^2\right) d\varphi \tag{47}$$

$$= 1 - 4\pi^2 \left[\frac{r}{\lambda}\right]^2 + o\left(\left[\frac{r}{\lambda}\right]^2\right) \tag{48}$$

The product of expressions (48) and (44) results in $1 + o\left(\left[\frac{r}{\lambda}\right]^2\right)$, which means that (48) is the inverse of (44), for small r/λ. This completes the proof of Corollary 1. $\square$

For a point-aperture, the limiting degrees of freedom function satisfies $\Omega(G) = 1$, which can be verified either directly from the definition (22), of alternatively, from (44) and $r = 0$. As the point-aperture starts to grow, Corollary 1 states that the increase in limiting degrees of freedom is in fact quadratic with the radius! Numerical results in Figure 4 indicate that the approximation from Corollary 1 remains valid up to $r = \lambda/4$.

Finally, using Corollary 1, we can provide simple estimates for area savings, which are achieved with dense multiantenna transceivers. For example, it is well-understood [1, 2] that obtaining two uncorrelated spatial dimensions for communication requires an array design which maintains a separation $2r = \lambda/2$ between the two antennas. An alternative to this design achieves $\Omega(G) = 2$ using (44) from Corollary 1, along with $4\pi^2 \left[r/\lambda\right]^2 = 1$. Hence, a dense multiantenna transceiver that satisfies $r < \lambda/6$ will provide two limiting degrees of freedom. This design alternative offers more than 50% savings in the array diameter, which can be accomplished using a total of three antennas (see $r = \lambda/7$ in Figure 4). Here, the cost of an additional antenna RF chain is required to compensate for the savings in the array diameter.

4.2.2 Approximation for Moderate-Sized Circular Arrays

To complete the study of limiting degrees of freedom for a circle, we next consider an important case of *moderate and large* circle radius r. For this purpose, Figure 6 depicts limiting degrees of freedom (33) as a function of r. In addition, Figure 6 also depicts a heuristic linear relationship $\Omega(G) \approx 2\pi \left[\frac{r}{\lambda}\right]$, which closely approximates limiting degrees of freedom by a circumference measured in carrier wavelengths. Explanation of this phenomenon is an open question, but consistent with a high-power study in [10].

Taking the signal-space approach, [10] considers the antenna array response to be the communication bottleneck, and shows that its basis contains approximately $4\pi \left[\frac{r}{\lambda}\right]$ functions, for large circle radius $r \gg \lambda$. Hence, for very high signal to noise ratios, circular antenna arrays can provide an increase in spectral efficiency of approximately $4\pi \left[\frac{r}{\lambda}\right]$ fold, when compared to single-input-single-output (SISO) transmission.

Approximation $\Omega(G) \approx 2\pi \left[\frac{r}{\lambda}\right]$ from Figure 6 suggests a similar conclusion for the low power regime, and in the range of *moderate-sized* apertures ($5\lambda - 100\lambda$). Namely, the baseline spectral efficiency of single-antenna Rayleigh fading channels is approximated with (3) and $\mathcal{S} = 2\kappa^{-1}(h) = 1$. Given a communication system with moderate-sized circular receiver aperture G, and with large effective degrees of freedom of the transmitter $\omega_{\mathrm{T}} \to \infty$, the spectral efficiency is approximated using $\mathcal{S} = 2\,\omega_{\mathrm{R}}(G) \approx 4\pi \left[\frac{r}{\lambda}\right]$. Therefore, the spectral efficiency which is achievable using circular G of radius r is approximately $4\pi \left[\frac{r}{\lambda}\right]$ multiple of spectral efficiency of SISO Rayleigh faded channels. We conjecture that the approximation $\Omega(G) \approx 2\pi \left[\frac{r}{\lambda}\right]$ also holds for *large-sized* circular arrays, but the behavior of $\Omega(G)$ in (33) for large $\frac{r}{\lambda}$ appears mathematically intractable.

Having observed a consistency between our work and the current literature [10], we conclude that linear relationship between limiting degrees of freedom and the circle radius holds valid only for moderate and possibly large-sized apertures. After presenting analytical results for the circle geometry, we now shift the discussion towards geometries with less symmetry but nonetheless equal practical importance, where we present numerical procedures and examples of configuration design.

5 Antenna Array Design Examples

5.1 Greedy Algorithm

In this section, we develop a simple greedy numerical procedure for antenna positioning, which will subsequently be used to optimize linear and square arrays below. The numerical procedure will perform a search over antenna configurations, with the goal of finding the one that maximizes the effective degrees of freedom (12). First, we briefly consider the *exhaustive configuration search,* which is optimal but computationally prohibitive, after which we introduce the alternative *greedy search,* which is suboptimal but with linear complexity.

Exhaustive search among all antenna configurations on the coordinate grid which covers G is clearly the optimal approach for configuration design. Unfortunately, even for small and fixed number of antennas, numerical complexity of the exhaustive search is exponential, because L hypothesis locations for M antennas results in $\binom{\mathrm{N}}{\mathrm{L}} \approx \mathrm{N}^{\mathrm{L}}$ computations of ω. For example, a relatively coarse $2-$dimensional search over a 10×10 grid with $\mathrm{M} = 10$ antennas results in approximately $\mathrm{N}^{\mathrm{L}} = 100^{10}$ computations of ω, which is too intensive for current generation computers.

Greedy search is a suboptimal but simple alternative to the exhaustive search. The main idea behind the greedy search is to start with an arbitrary antenna configuration, and successively increase ω by re-positioning a single antenna at a time. Pseudo-code for one iteration step of the greedy search is given below.
For antenna $m = \{1, .., \mathrm{M}\}$ do {

- Remove the $m-$th antenna from the current configuration.
- Fix the remaining $(\mathrm{M} - 1)$ antennas.
- Consider all $\mathrm{L} - (\mathrm{M} - 1)$ empty locations for the $m-$th antenna. Select the one which results in the overall configuration with maximum ω.

}.

Each iteration step of the greedy search consists of $\mathrm{M}(\mathrm{L} - \mathrm{M} + 1) < \mathrm{ML}$ evaluations of ω; hence, the aggregate complexity is approximately $\mathrm{ML}Q$ evaluations of ω, where Q is the number of iteration steps.

As previously noted, the greedy search for antenna configurations is suboptimum. The objective function ω has multiple extreme points, because all rotations of a certain antenna configuration result in the same effective degrees of freedom. Since the objective function has multiple extreme points, it must be non-convex (evidence for this is also provided by Figure 2 and Figure 3), and the greedy search algorithm may converge to a local maximum, depending on the initial antenna configuration. We therefore recommend running several trials with different initial configurations. Greedy configuration search is tested on linear and square arrays below, and results are compared against uniformly spaced antenna configurations.

5.2 Linear Arrays

Uniform linear arrays are the common benchmark case study for antenna configurations which are positioned on a straight line of length d. Figure 7 illustrates effective degrees of freedom for uniform linear arrays of various size and number of antennas. As predicted by Property 4 in Section 4.1, ω remains bounded, regardless of how many antennas are packed in a fixed-size array. We make several observations based on Figure 7.

Unlike for circular arrays, effective degrees of freedom of uniform linear arrays attain a peak at a finite number of antennas, which depends on the array size. For small-sized arrays where $d \leq 2\lambda$, the peak occurs at mutual antenna spacing of approximately $\lambda/4$, which is therefore recommended spacing for antennas which transmit/receive independent streams of data. For $d \leq 2\lambda$, effective degrees of freedom remain close to the upper bound given by uncorrelated arrays ($d = \infty$), before the peak occurs. Regardless of number of antennas, we report that greedy search algorithm converges to uniform configuration, given a small-sized array with $d \leq 2\lambda$.

The benefit of non-uniform configurations becomes apparent by considering moderate-sized apertures, such as $d = 4\lambda$. Here, the effective degrees of freedom function from Figure 7 grows very slow in the range from M = 6 to M = 9 antennas, which indicates suboptimality of uniform arrays. For these values of M, the greedy search converges to non-uniform antenna configurations, which are given in Figures 8 - 11. The comparison of effective degrees of freedom for uniform and non-uniform configurations, along with savings in spectral efficiency are given in Table 1. The largest saving in spectral efficiency (37%) is achieved for M = 8 antennas.

Size	Num. of Ant.	ω for Uniform	ω for Non-Uniform		Spec. Eff. Savings
$d = 4\lambda$	6	5.10	5.72	[Figure 8]	12%
$d = 4\lambda$	7	5.20	6.60	[Figure 9]	27%
$d = 4\lambda$	8	5.30	7.26	[Figure 10]	37%
$d = 4\lambda$	9	6.80	7.93	[Figure 11]	17%

Table 1: Comparison of uniform and non-uniform linear arrays.

Finally, as a conjecture based on data from Figure 7, we observe that for both moderate ($d = 4\lambda$) and large ($d = 20\lambda$ and $d = 40\lambda$) uniform linear arrays, effective degrees of freedom attain a peak at $\mathrm{M} = 2\left[\frac{d}{\lambda}\right] + 2$. For this particular value of M, the antenna spacing is $\frac{\lambda}{2+d^{-1}}$. Note that conventional $\frac{\lambda}{2}$ spacing leads to a uniform linear array of $\mathrm{M} = 2\left[\frac{d}{\lambda}\right] + 1$ antennas, which can incur a significant degradation in spectral efficiency (Figure 7), when compared to $\mathrm{M} = 2\left[\frac{d}{\lambda}\right] + 2$, which requires an additional antenna. As a practical conclusion, when constrained by the number of antennas and volume G, non-uniform arrays should be considered because they potentially offer substantial gains in spectral efficiency.

5.3 Square Arrays

In the final configuration design example, we consider positioning antennas on a square aperture G. Well-established benchmark configurations for square apertures are uniform square arrays, whose effective degrees of freedom are shown in Figure 12. The greedy search for antenna configurations is performed for a few sample values of aperture size and number of antennas, as reported in Table 2. Again, significant spectral efficiency savings are possible by simply considering non-uniform arrays, with no additional cost in number of antennas.

Size	Num. of Ant.	ω for Uniform	ω for Non-Uniform	Spec. Eff. Savings
d = $\frac{\lambda}{2}$	4	3.05	3.76 [Figure 13]	23%
d = λ	9	5.40	6.78 [Figure 14]	25%

Table 2: Comparison of uniform and non-uniform square arrays for array size of $d = 4\lambda$.

As a practical lesson, we emphasize that even conventionally popular design choices for antenna configurations may be substantially suboptimal, which in turn incurs a significant degradation in spectral efficiency. For example, a configuration of four antennas on a square aperture ($d = 0.5\lambda$) should not be positioned on the four vertices, and a greedy search algorithm has revealed a configuration in Figure 13, which improves spectral efficiency by whole 23%. Such improvements incur no penalty in terms of additional cost of hardware, or its complexity.

6 Conclusion

Key Concepts: Commercial-use devices for mobile communications are certainly limited by both size and by power consumption. Motivated by these practical constraints, this paper presents a study of performance limits for low power antenna arrays which are limited by a given wireless transceiver volume. Overall, key conceptual contributions were to quantify the effective degrees of freedom for a specific array configuration, and then to illustrate the concept of limiting degrees of freedom for a continuum of space $G \subseteq \mathbb{R}^3$. In this document, both concepts were applied to study circular, linear and square arrays, but their applicability extends beyond these examples. We believe that both effective and limiting degrees of freedom will find practical use in the hands of system architects, which are often requested to evaluate and synthesize antenna configurations.

Methodology: In practice, performance of antenna-array systems depends on multiple factors: the extent of channel scattering, availability of channel state information at transmitter and/or receiver, choice of transmission modality, antenna correlation, type of the antenna, mutual coupling, and finally operating point on the diversity-multiplexing tradeoff curve, to name a few. To manage the complexity of the impact of multiple co-existing factors, which possibly interact with each other, it is important to study how each of them contributes to the overall system performance. Towards this end, our current work targets basic understanding of the impact of limited volume on spectral efficiency. Naturally, always desirable approach is to characterize the relation between limited volume and spectral efficiency for all SNRs, but the general problem appears intractable at present. Fortunately, there is sufficient structure for approaching the problem at either very low or very high SNRs. [6]

As a final note, our approach is inspired by well-established information theoretic method of finding bounds using arbitrary but physically realizable systems. In particular, if specific array configuration is analogous to channel code with certain input distribution, then effective d.o.f. becomes analogous to its mutual information; furthermore, limiting d.o.f. can be regarded as "capacity" of a given space $G \subseteq \mathbb{R}^3$.

[6] Asymptotic performance analysis is typically much more manageable than finite parameter analysis.

Future Directions: Throughout this paper, he have repeatedly observed how the size limitation poses a relevant problem in terms of designing appropriate antenna configurations, and finding capacity tradeoffs of communication systems. This manuscript only scratches the surface of this problem, which is likely to partake a significant role in future applied research, in both information and communication theory. Many questions still remain open for future investigation. For example, a possible direction would be to relax the assumption of fully scattered arrays, and quantify the intuitive tradeoff between the amount of channel scattering and effective degrees of freedom. Potential answer to this question might come from combining results on various channel models and their impact on system capacity [9, 10, 20], and our results in this paper.

Finally, we note that this text documents the closed-form expression, as well as the computation methodology, for limiting d.o.f. of circular arrays. In addition, we conjecture that the analysis technique herein extends to spherical arrays as well. For linear and two-dimensional square arrays, the edge effects render the asymmetric correlation structure, which is why limiting d.o.f. does not appear to admit a closed form expression. For this reason, computing accurate approximations will be of great interest, primarily because of the prevalence of these geometries.

Appendix: Lemmas for Theorem 2

A Proof of Lemma 1

Proof. Direct computation yields

$$\mathrm{E}\left[\mathcal{H}\mathcal{H}^\dagger\right] = \mathrm{E}\left[\left(\Phi^{\frac{1}{2}}\widehat{\mathcal{H}}\Theta^{\frac{1}{2}}\right)\left(\Theta^{\frac{1}{2}}\widehat{\mathcal{H}}^\dagger\Phi^{\frac{1}{2}}\right)\right] \tag{49}$$

$$= \Phi^{\frac{1}{2}}\,\mathrm{E}\left[\widehat{\mathcal{H}}\Theta\widehat{\mathcal{H}}^\dagger\right]\Phi^{\frac{1}{2}}. \tag{50}$$

To proceed from (50), we will next use the standard eigenvalue decomposition of the transmit antenna correlation matrix $\Theta = Q\Lambda Q^\dagger$. Here, Λ is diagonal matrix which contains eigenvalues of Θ, and Q is unitary. This substitution gives

$$\mathrm{E}\left[\mathcal{H}\mathcal{H}^\dagger\right] = \Phi^{\frac{1}{2}}\,\mathrm{E}\left[\widehat{\mathcal{H}}\left(Q\,\Lambda Q^\dagger\right)\widehat{\mathcal{H}}^\dagger\right]\Phi^{\frac{1}{2}} \tag{51}$$

$$= \Phi^{\frac{1}{2}}\,\mathrm{E}\left[\widehat{\mathcal{H}}\Lambda\widehat{\mathcal{H}}^\dagger\right]\Phi^{\frac{1}{2}}. \tag{52}$$

Here, (52) holds because $\widehat{\mathcal{H}}$ is assumed to be isotropically invariant random matrix, which simply means that probability distribution of $\widehat{\mathcal{H}}$ is the same as probability distribution of $\widehat{\mathcal{H}}Q$ (for a unitary Q). This allows us to effectively eliminate Q from (51) and obtain (52).

To proceed from (52), we will evaluate the average of $\widehat{\mathcal{H}}\Lambda\widehat{\mathcal{H}}^\dagger$ on entry-by-entry basis. Because Λ is diagonal, it simply scales $n-$th column of $\widehat{\mathcal{H}}$ by $\Lambda(n, n)$. The entry (m, n) of $\widehat{\mathcal{H}}\Lambda$ therefore becomes $\widehat{\mathcal{H}}(m, n)\Lambda(n, n)$. Using the standard formula for (m, m') entry of matrix product $(\widehat{\mathcal{H}}\Lambda)\widehat{\mathcal{H}}^\dagger$, where brackets denote association, we have that (m, m') entry of the matrix $\widehat{\mathcal{H}}\Lambda\widehat{\mathcal{H}}^\dagger$ equals the following

$$\left.\widehat{\mathcal{H}}\Lambda\widehat{\mathcal{H}}^\dagger\right|_{(m,m')} = \sum_{n=1}^{\mathrm{N}} \widehat{\mathcal{H}}(m,n)\Lambda(n,n)\left[\widehat{\mathcal{H}}(m',n)\right]^\star, \tag{53}$$

where $\star$ denotes complex conjugate.

We will first focus on off-diagonal entries of $\widehat{\mathcal{H}}\Lambda\widehat{\mathcal{H}}^\dagger$, which are given by (53) and $m \neq m'$. The average of (53) equals 0 when $m \neq m'$, because $\widehat{\mathcal{H}}(n,m)$ is independent from $\widehat{\mathcal{H}}(m',n)$. On the other hand, for diagonal entries, where $m = m'$, the average of (53) equals $\mathrm{E}[|\widehat{h}|^2]\sum_n \Lambda(n,n)$. In summary, the average of the entire matrix $\widehat{\mathcal{H}}\Lambda\widehat{\mathcal{H}}^\dagger$ from (52) is in fact simply $\mathrm{E}[|\widehat{h}|^2]\mathrm{tr}(\Lambda)$ multiple of the identity. We therefore have

$$\begin{aligned}\mathrm{E}\left[\mathcal{H}\mathcal{H}^\dagger\right] &= \Phi\ [\mathrm{tr}\,\Lambda]\,\mathrm{E}\left[|\widehat{h}|^2\right] &(54)\\ &= \Phi\ [\mathrm{tr}\,\Theta]\,\mathrm{E}\left[|\widehat{h}|^2\right], &(55)\end{aligned}$$

where we used standard eigenvalue decomposition property $\mathrm{tr}(\Theta) = \mathrm{tr}(\Lambda)$. The last equality (55) completes the proof of Lemma 1. □

Finally, it is worthwhile noting that Lemma 1 is consistent with naming Φ the "receive antenna correlation." This remark is best illustrated by considering a scenario of single transmit - multiple receive antenna system, where $\mathcal{H}$ is $\mathrm{M} \times 1$ column vector. In this case, $\mathrm{E}\left[\mathcal{H}\mathcal{H}^\dagger\right]$ describes the $\mathrm{M} \times \mathrm{M}$ matrix of cross-correlations between propagation coefficients for each receive antenna, which is a scaled version of the Φ-matrix, according to the Lemma 1.

Lemma 1 essentially addresses the second-order average $\mathrm{E}\left[\mathcal{H}\mathcal{H}^\dagger\right]$ of the channel matrix $\mathcal{H}$. For the proof of Theorem 2 we also require the fourth order average of the channel matrix, which is the topic of Lemma 2.

B Proof of Lemma 2

Proof. Substituting $\Phi^{\frac{1}{2}}\widehat{\mathcal{H}}\Theta^{\frac{1}{2}}$ for $\mathcal{H}$ gives

$$\begin{aligned}\mathrm{E}\,\mathrm{tr}\left[\mathcal{H}\mathcal{H}^\dagger\mathcal{H}\mathcal{H}^\dagger\right] &= \mathrm{E}\,\mathrm{tr}\left[\left(\Phi^{\frac{1}{2}}\widehat{\mathcal{H}}\Theta^{\frac{1}{2}}\right)\left(\Theta^{\frac{1}{2}}\widehat{\mathcal{H}}^\dagger\Phi^{\frac{1}{2}}\right)\left(\Phi^{\frac{1}{2}}\widehat{\mathcal{H}}\Theta^{\frac{1}{2}}\right)\left(\Theta^{\frac{1}{2}}\widehat{\mathcal{H}}^\dagger\Phi^{\frac{1}{2}}\right)\right] &(56)\\ &= \mathrm{E}\,\mathrm{tr}\left[\widehat{\mathcal{H}}\Theta\widehat{\mathcal{H}}^\dagger\Phi\,\widehat{\mathcal{H}}\Theta\widehat{\mathcal{H}}^\dagger\Phi\right]. &(57)\end{aligned}$$

We note that deriving (57) from (56) requires three steps. First, it collects roots like $\Theta^{\frac{1}{2}}\Theta^{\frac{1}{2}} = \Theta$. Second, it moves $\Phi^{\frac{1}{2}}$ from left to right, using the fact that $\mathrm{tr}(B_1B_2) = \mathrm{tr}(B_2B_1)$. Third, it collects roots like $\Phi^{\frac{1}{2}}\Phi^{\frac{1}{2}} = \Phi$.

To proceed forward from (57), we will use eigenvalue decompositions of correlation matrices $\Theta = Q\Lambda Q^\dagger$ and of $\Phi = UDU^\dagger$. Here, both Λ and D matrices are diagonal and both Q and U are unitary. Substituting this into (57) yields

$$\begin{aligned}\mathrm{E}\,\mathrm{tr}\ \left[\mathcal{H}\mathcal{H}^\dagger\mathcal{H}\mathcal{H}^\dagger\right] &= \mathrm{E}\,\mathrm{tr}\ \left[\widehat{\mathcal{H}}\left(Q\Lambda Q^\dagger\right)\widehat{\mathcal{H}}^\dagger\left(UDU^\dagger\right)\ \widehat{\mathcal{H}}\left(Q\Lambda Q^\dagger\right)\widehat{\mathcal{H}}^\dagger\left(UDU^\dagger\right)\right] &(58)\\ &= \mathrm{E}\,\mathrm{tr}\ \left[\left(U^\dagger\widehat{\mathcal{H}}Q\right)\Lambda\left(Q^\dagger\widehat{\mathcal{H}}^\dagger U\right)D\left(U^\dagger\widehat{\mathcal{H}}Q\right)\Lambda\left(Q^\dagger\widehat{\mathcal{H}}^\dagger U\right)D\right] &(59)\end{aligned}$$

Notice that (59) is simply (58), where we moved $U^\dagger$ from right to left, again using the trace identity $\mathrm{tr}(B_1 B_2) = \mathrm{tr}(B_2 B_1)$. Terms are re-grouped in brackets in (59) because this grouping will make use of isotropical invariance of probability distribution on $\widehat{\mathcal{H}}$, which is the next step.

Under the assumption of isotropical invariance, the probability distribution of $\widehat{\mathcal{H}}$ is the same as the probability distribution of $U^\dagger \widehat{\mathcal{H}} Q$, because both U and Q matrices are unitary. We can therefore simplify (59) as follows

$$\mathrm{E}\,\mathrm{tr}\left[\mathcal{H}\mathcal{H}^\dagger\mathcal{H}\mathcal{H}^\dagger\right] = \mathrm{E}\,\mathrm{tr}\left[\widehat{\mathcal{H}}\Lambda\widehat{\mathcal{H}}^\dagger D\widehat{\mathcal{H}}\Lambda\widehat{\mathcal{H}}^\dagger D\right] \tag{60}$$

$$= \mathrm{E}\,\mathrm{tr}\left[\left(\widehat{\mathcal{H}}\Lambda\widehat{\mathcal{H}}^\dagger D\right)^2\right], \tag{61}$$

where (61) is nothing but an algebraic observation.

From (61), we will proceed to evaluate the average of $(\widehat{\mathcal{H}}\Lambda\widehat{\mathcal{H}}^\dagger D)^2$ on term-by-term basis. We utilize the expression (53) for (m, m') entry of $\widehat{\mathcal{H}}\Lambda\widehat{\mathcal{H}}^\dagger$, and since D is diagonal we have that (m, m') entry of $\widehat{\mathcal{H}}\Lambda\widehat{\mathcal{H}}^\dagger D$ equals

$$\left.\widehat{\mathcal{H}}\Lambda\widehat{\mathcal{H}}^\dagger D\right|_{(m,m')} = \sum_{n=1}^{N} \widehat{\mathcal{H}}(m,n)\Lambda(n,n)\left[\widehat{\mathcal{H}}(m',n)\right]^\star D(m',m'). \tag{62}$$

To address the square in (61) we note the following fact: if B is a generic M×M matrix, then each (m, m) entry of B^2 equals $\sum_{m'} B(m, m')B(m', m)$. From here we evaluate the trace of B^2 as $\mathrm{tr}(B^2) = \sum_{m,m'} B(m, m')B(m', m)$. With this and (62) we have that (61), without the averaging operator E, admits the following representation

$$\mathrm{tr}\left[\left(\widehat{\mathcal{H}}\Lambda\widehat{\mathcal{H}}^\dagger D\right)^2\right] = \sum_{m}\sum_{m'}\sum_{n}\sum_{n'}$$

$$\widehat{\mathcal{H}}(m,n)\Lambda(n,n)\left[\widehat{\mathcal{H}}(m',n)\right]^\star D(m',m')\widehat{\mathcal{H}}(m',n')\Lambda(n',n')\left[\widehat{\mathcal{H}}(m,n')\right]^\star D(m,m) \tag{63}$$

To complete the proof of this lemma, we must evaluate the average of (63). Here, we will separately consider four possible cases of relationships between m' and m, and n' and n.

Case 1 [$m \neq m'$ and $n \neq n'$] : For this trivial case, the average of (63) equals 0. This conclusion holds due to the zero-mean and independence assumption on entries $\widehat{\mathcal{H}}(m, n)$.

Case 2 [$m = m'$ and $n = n'$] : The average of (63) now equals

$$\mathrm{E}\left[\sum_{m}\sum_{n}\left|\widehat{\mathcal{H}}(m,n)\right|^4 |\Lambda(n,n)|^2\,|D(m,m)|^2\right] = \mathrm{E}\left[|\widehat{h}|^4\right]\mathrm{tr}\left[\Lambda^2\right]\mathrm{tr}\left[D^2\right] \tag{64}$$

$$= \mathrm{E}\left[|\widehat{h}|^4\right]\mathrm{tr}\left[\Phi^2\right]\mathrm{tr}\left[\Theta^2\right]. \tag{65}$$

The last equality (65) is true, because $\mathrm{tr}\left(\Phi^2\right) = \mathrm{tr}\left(Q\Lambda Q^\dagger Q\Lambda Q^\dagger\right) = \mathrm{tr}\left(\Lambda^2\right)$, which in turn holds because Q is unitary matrix.

Case 3 $[m = m'$ and $n \neq n']$: Here, (63) gives

$$\sum_{m} \sum_{\substack{n,n' \\ n \neq n'}} \mathrm{E}\left[\left|\widehat{\mathcal{H}}(m,n)\right|^2\right] \mathrm{E}\left[\left|\widehat{\mathcal{H}}(m,n')\right|^2\right] \Lambda(n,n) \left|D(m,m)\right|^2 \Lambda(n',n') \tag{66}$$

$$= \mathrm{E}\left[|\widehat{h}|^2\right]^2 \sum_{m} |D(m,m)|^2 \sum_{\substack{n,n' \\ n \neq n'}} \Lambda(n,n)\Lambda(n',n') \tag{67}$$

Notice that the last double summation over n and n' is in fact a square of $\sum_n \Lambda(n,n)$, except for the terms when $n = n'$. To complete the third case, (67) will be expressed as

$$\mathrm{E}\left[|\widehat{h}|^2\right]^2 \operatorname{tr}\left(D^2\right) \left[\left[\sum_{n,n'} \Lambda(n,n)\Lambda(n',n')\right] - \sum_{n} \Lambda^2(n,n)\right] \tag{68}$$

$$= \mathrm{E}\left[|\widehat{h}|^2\right]^2 \operatorname{tr}\left[D^2\right] \left[[\operatorname{tr}\Lambda]^2 - \operatorname{tr}\left[\Lambda^2\right]\right] \tag{69}$$

$$= \mathrm{E}\left[|\widehat{h}|^2\right]^2 \operatorname{tr}\left[\Theta^2\right] \left[[\operatorname{tr}\Phi]^2 - \operatorname{tr}\left[\Phi^2\right]\right]. \tag{70}$$

Case 4 $[m \neq m'$ and $n = n']$: This case is similar to the previous one. Hence, by symmetry, we may interchange Φ and Θ in (70) to arrive at

$$\mathrm{E}\left[|\widehat{h}|^2\right]^2 \operatorname{tr}\left[\Phi^2\right] \left[[\operatorname{tr}\Theta]^2 - \operatorname{tr}\left[\Theta^2\right]\right]. \tag{71}$$

To compute the desired average of (63), we combine all three non-trivial cases (2 - 4), starting from (65), then (70), and finally (71). The addition of these three terms provides desired sum from Lemma 2, which complets its proof. $\square$

References

[1] I.E.Telatar, "Capacity of Multi-Antenna Gaussian Channels," Bell Labs Internal Technical Memo., June 1995.

[2] G.J. Foschini and M.J. Gans, "On Limits of Wireless Communication in a Fading Environment when Using Mulitple Antennas", *"Wireless Personal Communications,"* pp. 311 - 335, March 1998.

[3] S. Verdu, "Spectral Efficiency in the Wideband Regime," *IEEE Transactions on Information Theory,* vol. 48, pp. 1319 - 1343, June 2002.

[4] Special Issue on MIMO Systems, *IEEE Trans. on Information Theory,* Oct. 2003.

[5] W. C. Jakes, Jr., "Microwave Mobile Communications," New York: Wiley, 1974.

[6] C. Cuah, D. Tse, J. Kahn and R. Valenzuela, "Capacity Scaling in MIMO Wireless systems Under Correlated Fading," *IEEE Transactions on Information Theory,* vol. 48, no. 3, pp.637-650, March 2002.

[7] A. Lozano, A. Tulino and S. Verdu, "Multiantenna Capacity in the Low-Power Regime," *IEEE Transactions on Information Theory,* Vol 49, no. 10, pp. 2527-2544, Oct. 2003.

[8] T. S. Pollock, T. D. Abhayapala and R. A. Kennedy, "Antenna Saturation Effects on Dense Array MIMO Capacity," Proceedings of ICASSP 2003 - Hong Kong.

[9] T. S. Pollock, T. D. Abhayapala and R. A. Kennedy, "Limits to Multi-Antenna Capacity of Spatially Selective Channels," Proceedings of ISIT 2004 - Chicago.

[10] Ada Poon, R. Brodersen and D. Tse, "Degrees of Freedom in Multiple Antenna Channels: A Signal Space Approach," *Submitted to IEEE Transactions on Information Theory.*

[11] N. Chiurtu, B. Rimoldi and Emre Telatar, "Impact of Correlation and Coupling on The Capacity of MIMO Systems," Proceedings of ISSPIT 2003 - Darmstadt.

[12] D. Gesbert, T. Eikman and N Christophersen, "Capacity Limits of Palm-Sized MIMO Arrays," Proceedings of Globecomm 2003 - San Francisco.

[13] J. G. Proakis, "Digital Communications," New York: McGraw-Hill, 1995.

[14] T. M. Cover and J. A. Thomas, "Elements of Information Theory," New York: Wiley, 1991.

[15] T. Marzetta and B. Hochwald, "Capacity of mobile multiple-antenna communication link in a Rayleigh flat-fading environment," *IEEE Transactions on Information Theory,* vol. 45, pp.139-157, Jan. 1999.

[16] V.V. Prasolov, "Problems and Theorems in Linear Algebra," American Mathematical Society, 1994.

[17] J. Wallace and M. Jensen, "Mutual Coupling in MIMO Wireless Systems: A Rigorous Network Theory Analysis," *IEEE Transactions on Wireless Communications,* Vol 3, no. 4, pp. 1317-1325, July 2004.

[18] M. Rupf and J. L. Massey, "Optimum sequence multisets for synchronous code-division multiple-access channels," *IEEE Transactions on Information Theory,* Vol. 40, pp. 1261-1266, July 1994.

[19] T. Muharemovic, A. Sabharwal and B. Aazhang, "On limits of Antenna Packing in Low Power Systems," Proceedings of the Forty-Second Annual Allerton Conference on Communication, Control, and Computing, Sept. 2004.

[20] K. Liu, V. Raghavan and A. Sayeed, "Capacity Scaling and Spectral Efficiency of Wide-Band Correlated MIMO Channels," *IEEE Transactions on Information Theory,* vol. 49, pp.2504-2526, Oct. 2003.

[21] D. Chizhik, F. R. Farrokhi, J. Ling, and A. Lozano, "Effect of antenna separation on the capacity of BLAST in correlated channels," *IEEE Communications Letters,* Vol. 4, pp. 337 - 339, Nov. 2000.

[22] H. E. Gamal and A. R. Hammons Jr., "A new approach to layered space-time coding and signal processing," *IEEE Transactions on Information Theory,* Vol. 47, pp. 2321 - 2334, Sept. 2001.

[23] D. J. Love, R. W. Heath, Jr., and T. Strohmer, "Grassmannian beamforming for multiple-input multiple-output wireless systems," *IEEE Transactions on Information Theory,* 49(10), pp. 2735 - 2747, Oct. 2003.

[24] B. Hassibi and B. M. Hochwald, "High-rate codes that are linear in space and time," *IEEE Transactions on Information Theory,* Vol. 48, pp. 1804 - 1824, July 2002.

[25] L. Zheng and D. N. C. Tse, "Diversity and Multiplexing: A Fundamental Tradeoff in Multiple Antenna Channels," *IEEE Transactions on Information Theory,* Vol. 49, pp. 1073 - 1096, May 2003.

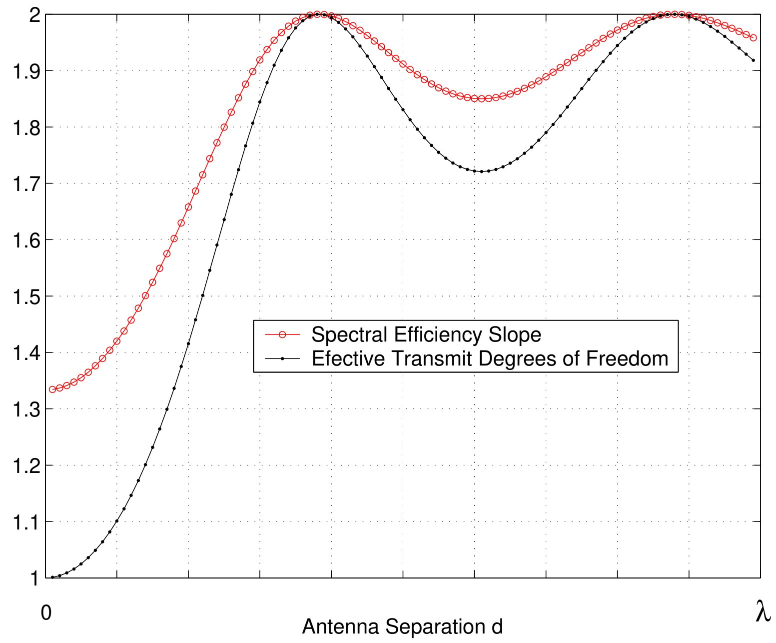

Figure 1: Spectral efficiency slope and effective transmit degrees of freedom for a 2×2 MIMO system: correlated transmitter and fully uncorrelated receiver.

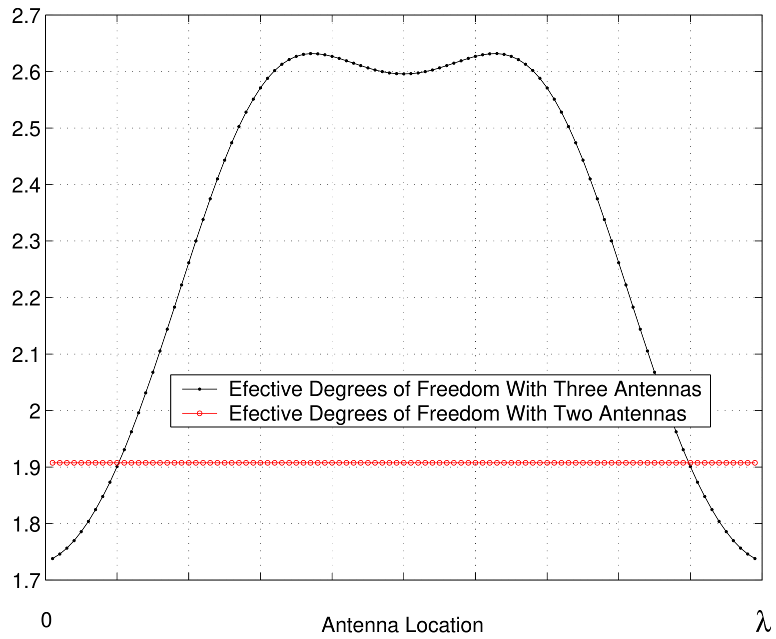

Figure 2: Effective degrees of freedom as a function of distance between first and second antenna element in a 3-element linear array; length of the array is λ.

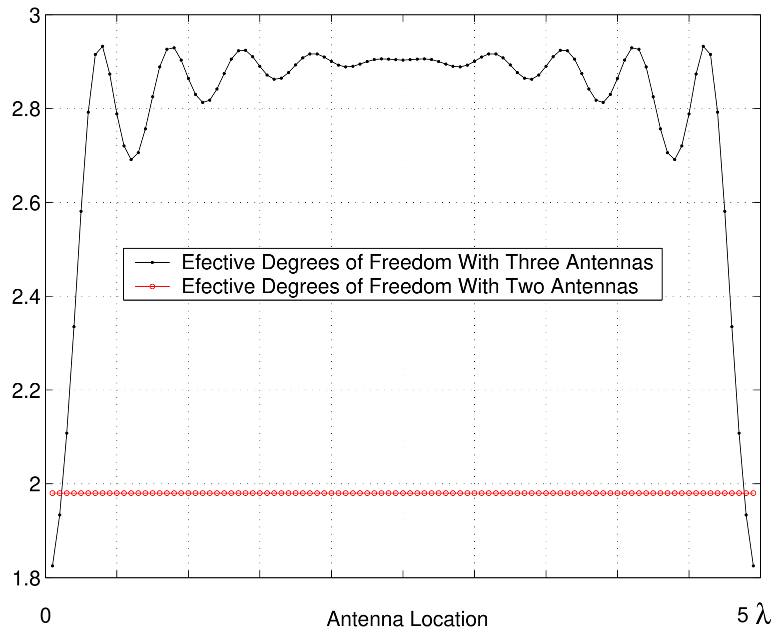

Figure 3: Effective degrees of freedom as a function of distance between first and second antenna element in a 3-element linear array; length of the array is 5λ.

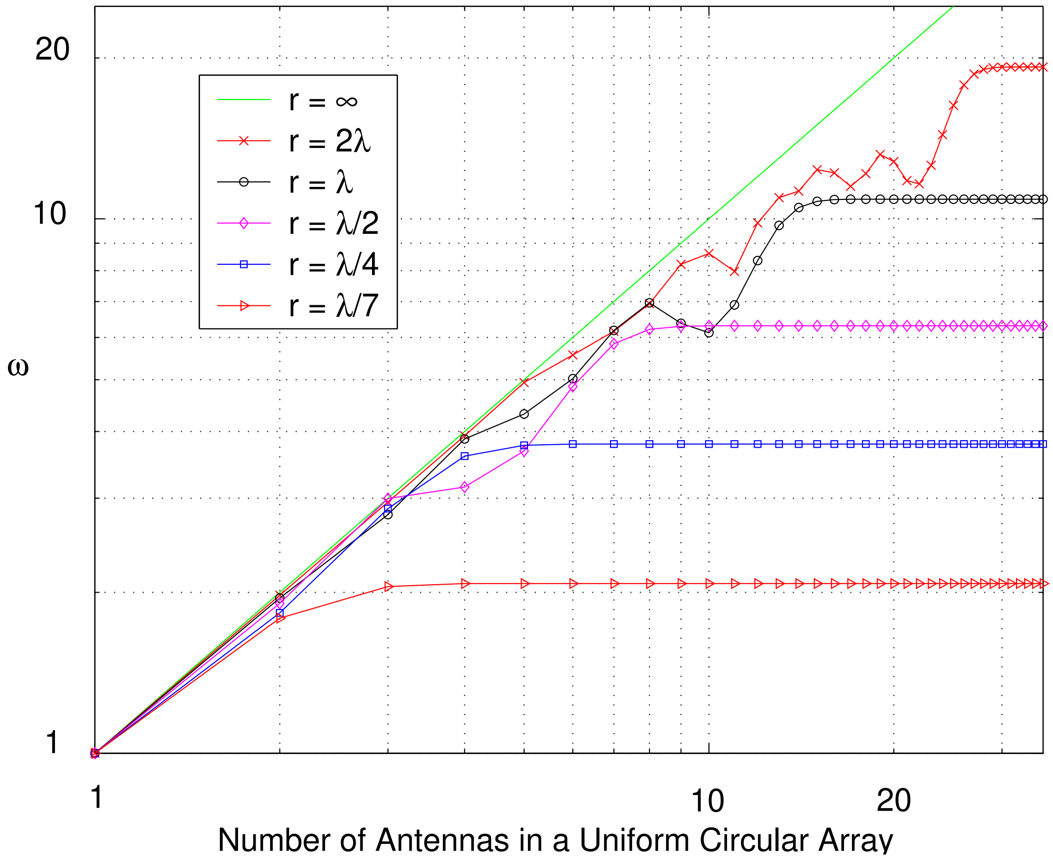

Figure 4: Effective degrees of freedom versus the number of antenna elements in a uniform circular array; radius of the array is r.

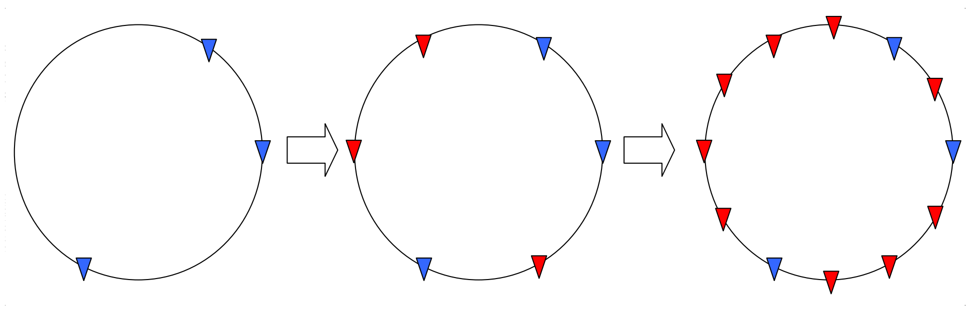

Figure 5: An illustration which is used for the proof of Theorem 3.

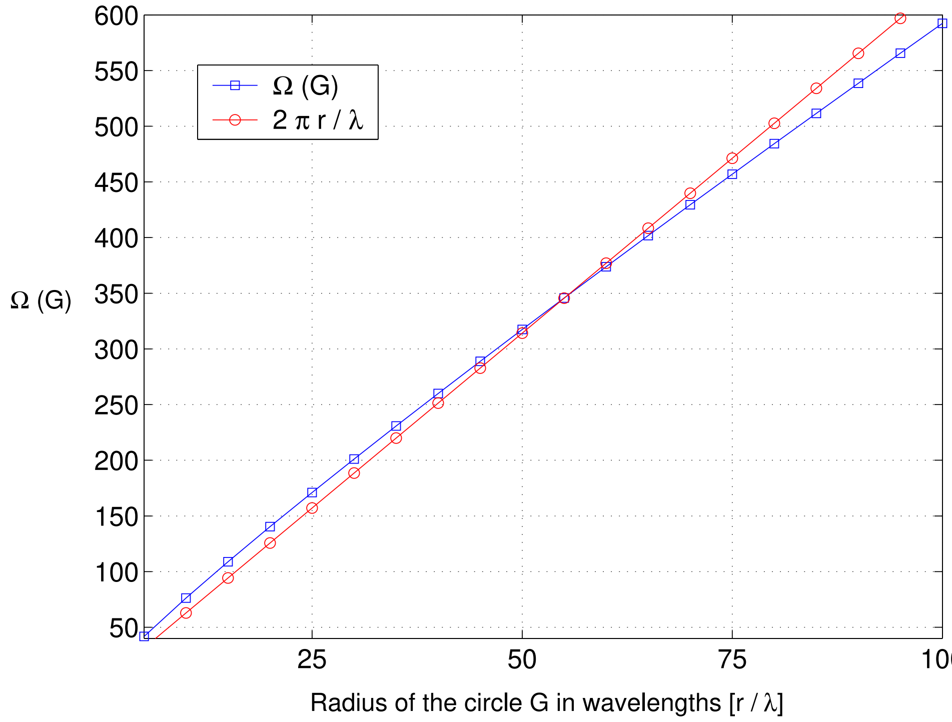

Figure 6: Limiting degrees of freedom and the linear approximation, for a circle.

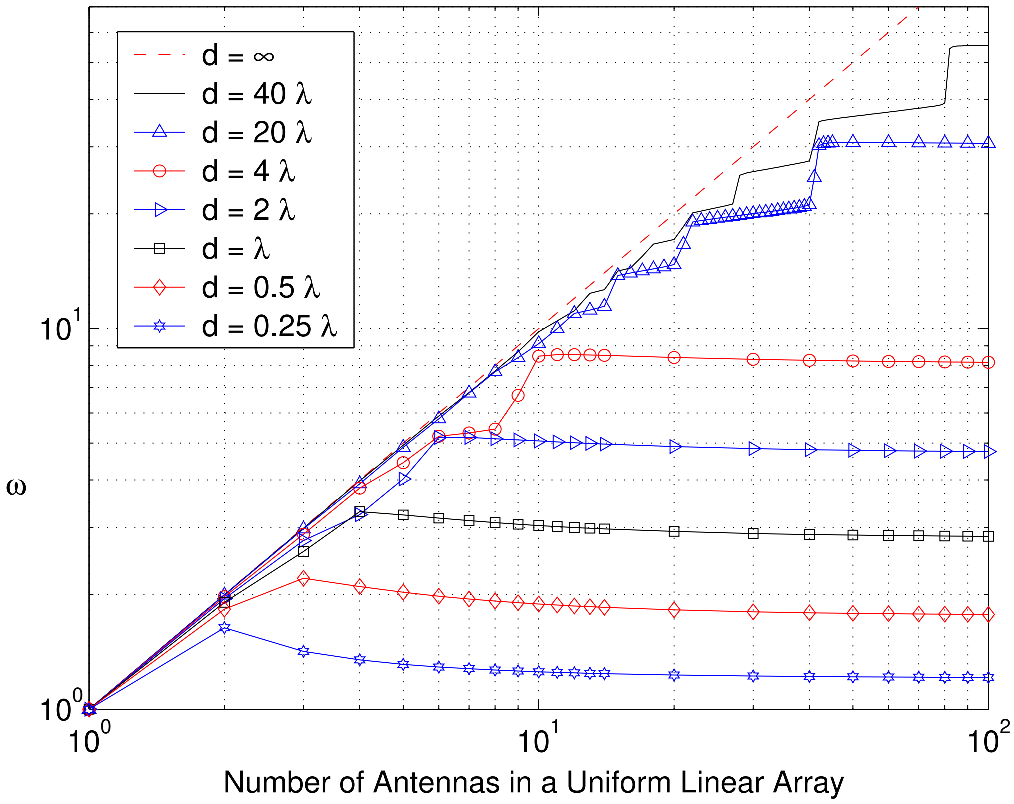

Figure 7: Effective degrees of freedom versus the number of antenna elements in a uniform linear array; length of the array is d.

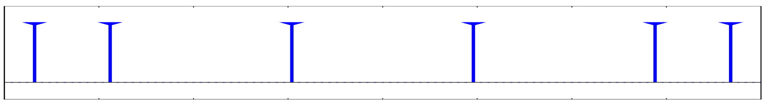

Figure 8: Array which offers 12% improvement in spectral efficiency over the uniform. Antenna locations are $\begin{bmatrix}0.04 & 0.14 & 0.38 & 0.62 & 0.86 & 0.96\end{bmatrix} \times 4\,\lambda$.

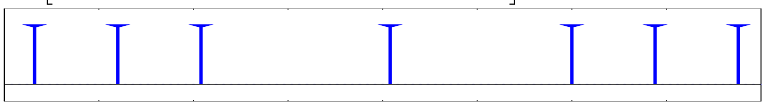

Figure 9: Array which offers 27% improvement in spectral efficiency over the uniform. Antenna locations are $\begin{bmatrix}0.04 & 0.15 & 0.26 & 0.51 & 0.75 & 0.86 & 0.97\end{bmatrix} \times 4\,\lambda$.

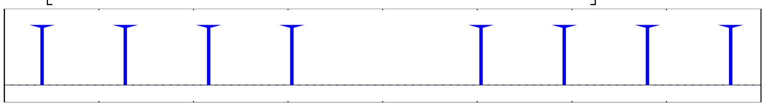

Figure 10: Array which offers 37% improvement in spectral efficiency over the uniform. Antenna locations are $\begin{bmatrix}0.05 & 0.16 & 0.27 & 0.38 & 0.63 & 0.74 & 0.85 & 0.96\end{bmatrix} \times 4\,\lambda$.

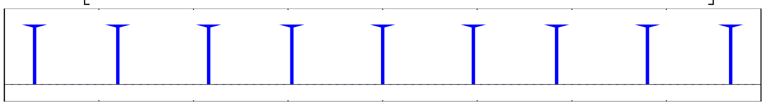

Figure 11: Array which offers 17% improvement in spectral efficiency over the uniform. Antenna locations are $\begin{bmatrix}0.04 & 0.15 & 0.27 & 0.38 & 0.50 & 0.62 & 0.73 & 0.85 & 0.96\end{bmatrix} \times 4\,\lambda$.

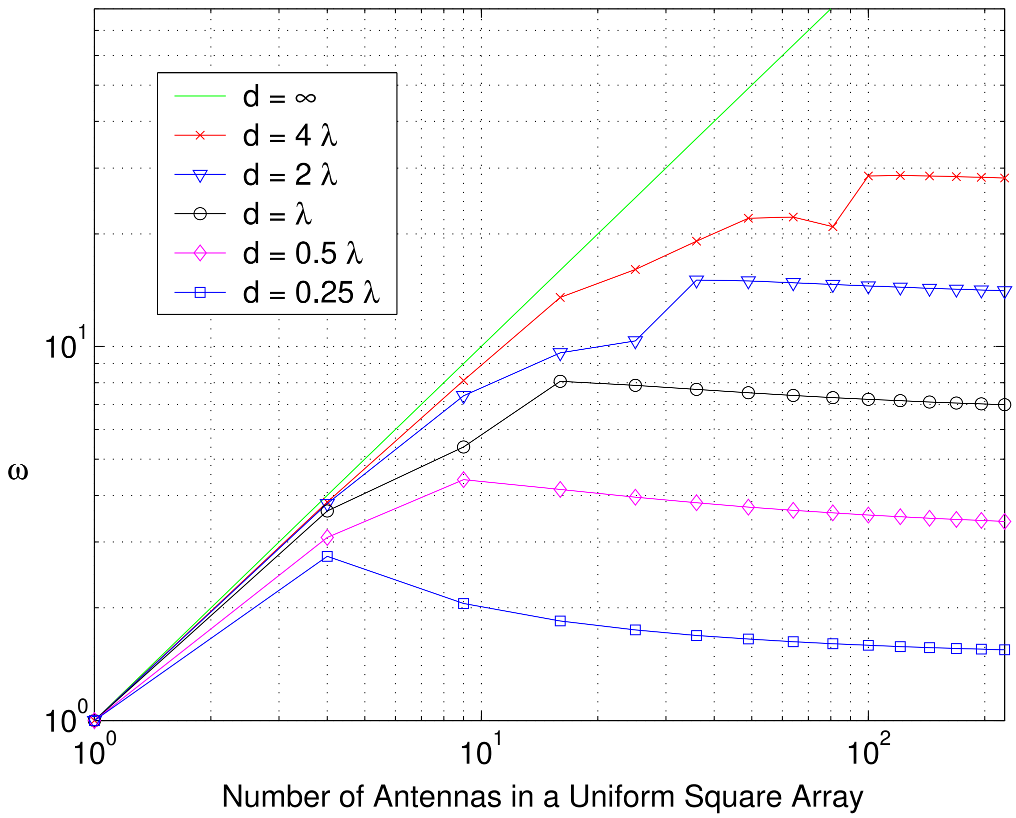

Figure 12: Effective degrees of freedom versus the number of antenna elements in a uniform square array; edge of the array is d.

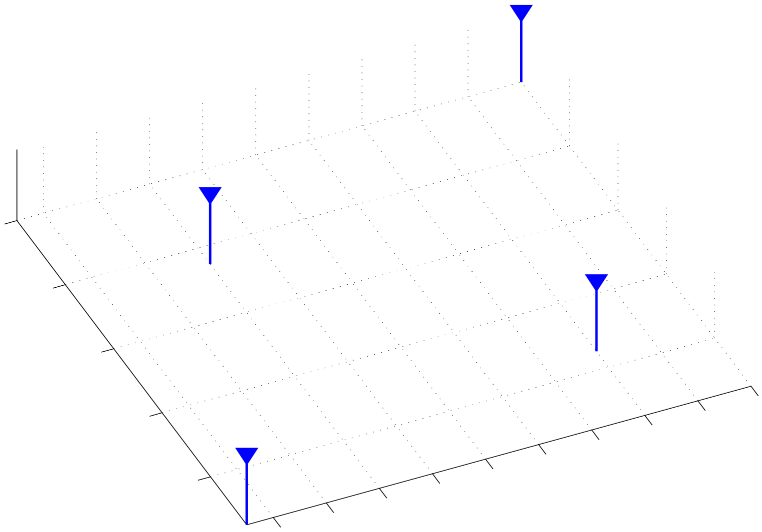

Figure 13: Array which offers 23% improvement in spectral efficiency over the uniform. Antenna locations are $\begin{bmatrix} (0.00, 0.00) & (1.00, 1.00) & (0.74, 0.26) & (0.21, 0.79) \end{bmatrix} \times \frac{\lambda}{2}$.

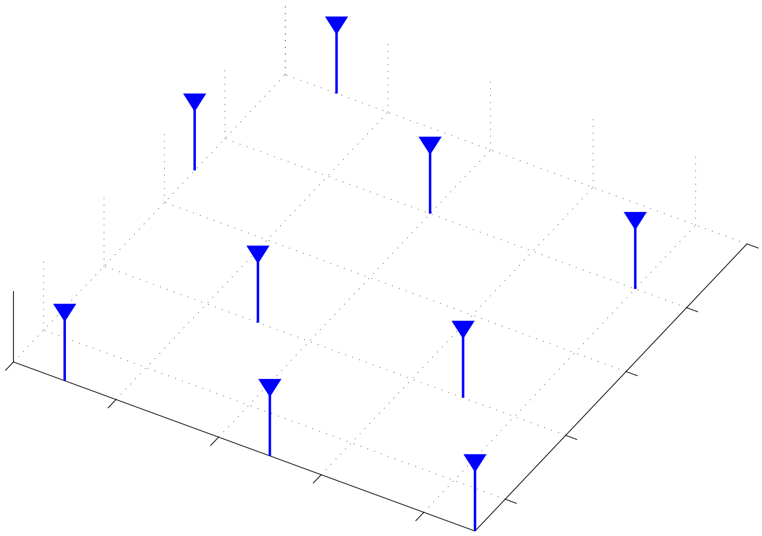

Figure 14: Array which offers 25% improvement in spectral efficiency over the uniform. Antenna locations are $\begin{bmatrix} (0.00, 0.00) & (0.00, 0.44) & (0.00, 0.89) & (0.33, 0.22) \\ (0.33, 0.66) & (0.67, 1.00) & (0.78, 0.11) & (0.78, 0.56) & (1.00, 0.89) \end{bmatrix} \times \lambda$.